IAI Journals.ASM.org

Parasite Manipulation of the Invariant Chain and the Peptide Editor H2-DM Affects Major Histocompatibility Complex Class II Antigen Presentation during *Toxoplasma gondii* Infection

Louis-Philippe Leroux,[a] Manami Nishi,[a] Sandy El-Hage,[a] Barbara A. Fox,[b] David J. Bzik,[b] Florence S. Dzierszinski[a,c]

Institute of Parasitology, McGill University, Sainte-Anne-de-Bellevue, Québec, Canada[a]; Geisel School of Medicine at Dartmouth, Lebanon, New Hampshire, USA[b]; Carleton University, Ottawa, Ontario, Canada[c]

***Toxoplasma gondii* is an obligate intracellular protozoan parasite. This apicomplexan is the causative agent of toxoplasmosis, a leading cause of central nervous system disease in AIDS. It has long been known that *T. gondii* interferes with major histocompatibility complex class II (MHC-II) antigen presentation to attenuate CD4$^+$ T cell responses and establish persisting infections. Transcriptional downregulation of MHC-II genes by *T. gondii* was previously established, but the precise mechanisms inhibiting MHC-II function are currently unknown. Here, we show that, in addition to transcriptional regulation of MHC-II, the parasite modulates the expression of key components of the MHC-II antigen presentation pathway, namely, the MHC-II-associated invariant chain (Ii or CD74) and the peptide editor H2-DM, in professional antigen-presenting cells (pAPCs). Genetic deletion of CD74 restored the ability of infected dendritic cells to present a parasite antigen in the context of MHC-II *in vitro*. CD74 mRNA and protein levels were, surprisingly, elevated in infected cells, whereas MHC-II and H2-DM expression was inhibited. CD74 accumulated mainly in the endoplasmic reticulum (ER), and this phenotype required live parasites, but not active replication. Finally, we compared the impacts of genetic deletion of CD74 and H2-DM genes on parasite dissemination toward lymphoid organs in mice, as well as activation of CD4$^+$ T cells and interferon gamma (IFN-γ) levels during acute infection. Cyst burdens and survival during the chronic phase of infection were also evaluated in wild-type and knockout mice. These results highlight the fact that the infection is influenced by multiple levels of parasite manipulation of the MHC-II antigen presentation pathway.**

Toxoplasma gondii is an obligate intracellular protozoan parasite with a remarkable host range consisting of all warm-blooded vertebrates, including humans and mice (1, 2). During acute infection, rapidly dividing tachyzoites primarily disseminate throughout the host and infect any nucleated cell, including cells of the immune system, in which they replicate within a parasitophorous vacuole (PV) (3). Shortly after infection, *T. gondii* parasites reach immune-privileged sites, such as the brain and muscle tissues, and convert to latent bradyzoites, which encyst to persist throughout the host's life. Encystation can occur as early as 6 to 9 days postinfection (p.i.) (4), timing concomitant with the development of a potent parasite-specific adaptive immune response. Although toxoplasmosis is generally asymptomatic in healthy individuals, congenital toxoplasmosis can lead to serious birth defects, such as hydrocephaly, mental retardation, blindness, and chorioretinitis (5). Furthermore, reactivation of encysted parasites represents a serious threat to immunosuppressed individuals, such as AIDS patients and individuals receiving chemotherapy against cancer or immunosuppressive drugs during organ transplantation, and to elderly people with an aging immune system (3, 6).

In immunocompetent hosts, resistance against *T. gondii* is characterized by a robust Th1-type response that is mediated by the cellular arm of the immune system, namely, CD8$^+$ and CD4$^+$ T cells, which provide protective immunity through the production of IFN-γ (7–9). Despite the induction of a strong immune response, the infection inevitably reaches the chronic stage as the parasite encysts. It has been reported that *T. gondii* utilizes different mechanisms to subvert several immune functions, including the inhibition of proinflammatory signaling cascades, such as NF-κB (10), MAPK (11), STAT1 (12–14), and CIITA (15); induction of anti-inflammatory STAT3/6-mediated transcription (16–18); and inhibition of immunity-related GTPase (IRG)-mediated destruction of the PV (19–21). Furthermore, it has been shown that *T. gondii* interferes with antigen presentation in the context of major histocompatibility complex class II (MHC-II) (22–24), which is required for priming and activation of CD4$^+$ T cells (25).

MHC-II glycoproteins are synthesized in the endoplasmic reticulum (ER), where they associate with the MHC-II-associated invariant-chain (Ii or CD74) chaperone to form a nonameric complex, where three MHC-II chain dimers (an α and a β chain) associate with CD74 trimers (26, 27). Professional antigen-presenting cells (pAPCs), such as macrophages, dendritic cells (DCs), and B cells, readily express MHC-II molecules, and their expression is upregulated by proinflammatory stimuli (25). The invari-

Received 20 April 2015 **Returned for modification** 13 May 2015
Accepted 11 July 2015

Accepted manuscript posted online 20 July 2015

Citation Leroux L-P, Nishi M, El-Hage S, Fox BA, Bzik DJ, Dzierszinski FS. 2015. Parasite manipulation of the invariant chain and the peptide editor H2-DM affects major histocompatibility complex class II antigen presentation during *Toxoplasma gondii* infection. Infect Immun 83:3865–3880. doi:10.1128/IAI.00415-15.

Editor: J. H. Adams

Address correspondence to Florence S. Dzierszinski, florence.dzierszinski@carleton.ca.

L.-P.L. and M.N. contributed equally to this work.

Supplemental material for this article may be found at http://dx.doi.org/10.1128/IAI.00415-15.

doi:10.1128/IAI.00415-15

ant chain, a nonpolymorphic type II membrane protein, prevents nonspecific loading of peptides onto MHC-II molecules by occupying the MHC-II groove. In addition, CD74 contains dileucine-based sorting motifs within its cytoplasmic region (28, 29) that are recognized by either AP1 and AP3, or AP2, adaptor proteins, which direct trafficking of CD74/MHC-II complexes to the cell surface as immature complexes or to the endocytic pathway for maturation from the *trans*-Golgi network (TGN), respectively (30, 31). Within acidified late endosomal compartments, resident aspartic and cysteine proteases (i.e., legumain and cathepsins), which require an acidic environment for autocatalytic activation and optimal activity, break down antigens into small antigenic peptides and also cleave CD74 in a sequential manner to yield the class II-associated invariant-chain peptide (CLIP) associated with the MHC-II groove (32). CLIP is thereafter displaced by the peptide editor H2-DM (or HLA-DM in humans), an MHC-II-like molecule, and a higher-affinity antigenic peptide is loaded onto the mature MHC-II molecule. This complex is finally brought to the surface to be presented to $CD4^+$ T cells bearing a cognate receptor (T cell receptor [TCR]).

Previous studies have reported transcriptional regulation of MHC-II and other, related genes in *Toxoplasma*-infected cells, whereby interferon gamma (IFN-γ)-induced transcription is inhibited in infected cells (15, 33, 34). Levels of MHC-II proteins are reduced in infected cells, antigen presentation is impaired, and priming and activation of $CD4^+$ T cells are greatly diminished (23, 24, 35), yet small amounts of MHC-II proteins are detected in these cells. Others have reported opposing views, where *Toxoplasma* activates human blood DCs upon invasion (36) and soluble *T. gondii* antigens (STAg) activate murine splenic $CD8\alpha^+$ DCs (37–40). Currently, it is not known if the defect in MHC-II antigen presentation can be attributed primarily to the reduced expression of MHC-II during *T. gondii* infection.

The aim of this study was to assess the impact of *T. gondii* infection on key components of the MHC-II antigen presentation pathway, specifically, the regulation of CD74 and H2-DM expression. Here, we show that CD74 expression is not coordinated at either the transcript or the protein level with that of MHC-II and H2-DM in *T. gondii*-infected pAPCs. CD74 expression was strongly induced by the parasite in the absence of exogenous IFN-γ or endogenous type I IFNs and tumor necrosis factor alpha (TNF-α), and parasite induction of CD74 prevented MHC-II-dependent presentation of endogenously acquired, parasite-derived antigens. In addition, the impacts of genetic deletion of CD74 and H2-DM during acute and chronic infections were assessed, specifically those on parasite dissemination toward lymphoid organs, $CD4^+$ T cell activation, IFN-γ levels, and cyst burdens and survival in infected mice. In addition, opposing expression patterns of CD74 and H2-DM were found to affect parasite dissemination toward lymphoid organs, activation of $CD4^+$ T cells, and production of IFN-γ during acute infection and to significantly influence cyst burdens in the chronic phase of infection.

MATERIALS AND METHODS

Mice. Animal procedures were conducted in accordance with the guidelines and policies of the Canadian Council on Animal Care. All animals were housed and maintained according to the guidelines of the McGill University Animal Care Committee (permit AUC 5380), and all efforts were made to minimize discomfort and suffering of the animals during the study. Four- to 6-week-old wild-type (WT) C57BL/6 and BALB/c mice were purchased from Charles River Laboratory (Wilmington, MA). CD74 knockout (KO) ($CD74^{-/-}$) mice in the BALB/c [CAn.129S6(B6)-*Ii*^{tm1Liz}/J] and C57BL/6 (B6.129S6-*Ii*^{tm1Liz}/J) backgrounds (41) and H2-DM KO ($H2\text{-}DM^{-/-}$) mice (B6.129S4-*H2-DMa*^{tm1Doi}/J) in the C57BL/6 background (42) were purchased from Jackson Laboratory (Bar Harbor, ME) and bred in house. Double-knockout (dKO) ($CD74^{-/-}$ $H2\text{-}DM^{-/-}$) animals were generated by cross-breeding $CD74^{-/-}$ and $H2\text{-}DM^{-/-}$ lines and cross-breeding the progeny for three generations; the genotype was confirmed by PCR with primers designed for mutated alleles (see Table S1 in the supplemental material). Also, hind leg bones from $CD74^{-/-}$ mice in the C57BL/6 background (kindly provided by Elizabeth Bikoff [University of Oxford]) were used to generate bone marrow-derived pAPCs.

Parasite and host cell cultures. Type I virulent *T. gondii* cultures of the RH strain (WT and transgenic) and type II avirulent Prugniaud (Pru) Δ*hgxprt* (hypoxanthine-guanine-xanthine phosphoribosyltransferase) tachyzoites (kind gifts from D. Soldati-Favre [University of Geneva]) were maintained by serial passages in human foreskin fibroblasts (HFF) (ATCC, Manassas, VA), as previously described (43).

The carbamoyl phosphate synthetase II deletion mutant (Δ*cpsII*) (44) was maintained in culture in the presence of exogenous uracil (0.2 mM). Transgenic parasite clonal lines were engineered to express the fluorescent markers red fluorescent protein (RFP) (DsRed; BD Clontech, Palo Alto, CA) in the cytosol and yellow fluorescent protein (YFP) secreted into the PV or, in the Δ*cpsII* background, the model antigen Eα (I-Eα peptide from the BALB/c haplotype [45]) fused to RFP in the cytosol or secreted into the PV. The *ptub*-RFP/*sag*CAT and *ptub*P30-YFP/*sag*CAT plasmids (46) and the *ptub*Eα-RFP/*sag*CAT and *ptub*P30-Eα-RFP/*sag*CAT plasmids (47) were described previously.

Bone marrow-derived macrophages (BMMϕ) and dendritic cells (BMDCs) were obtained by differentiating precursor cells from murine bone marrow as previously described (48, 49). Briefly, mice were euthanized by CO_2 asphyxiation, and hind legs were collected in Dulbecco's modified Eagle's medium (DMEM). The marrow was flushed out of the bones, and live precursor cells were counted using trypan blue exclusion staining. For BMMϕ, 5×10^6 precursor cells were resuspended in culture medium (DMEM, 10% fetal bovine serum [FBS], 2 mM L-glutamate, 1,000 U/ml penicillin, 1,000 μg/ml streptomycin, 50 μg/ml gentamicin, 2.5% HEPES, 55 μM beta-mercaptoethanol, 1 mM sodium pyruvate [Wisent, St-Bruno, Quebec, Canada]) supplemented with 30% L929 fibroblast-conditioned medium, and the cells were seeded in 10-cm petri dishes. The medium was changed 3 days later. Differentiated BMMϕ were used in assays 8 days after bone marrow harvest. Expression of the CD11b marker was assessed by flow cytometry to confirm differentiation. BMDCs were produced by culturing 2×10^6 precursor cells in complete culture medium (RPMI, 10% FBS, 2 mM L-glutamate, 1,000 U/ml penicillin, 1,000 μg/ml streptomycin, 50 μg/ml gentamicin, 2.5% HEPES, 55 μM beta-mercaptoethanol) supplemented with 40 ng/ml of recombinant granulocyte-macrophage colony-stimulating factor (rGM-CSF) and 10 ng/ml recombinant interleukin 4 (rIL-4) (Peprotech, Rocky Hill, NJ) in 10-cm petri dishes. Feeding medium was added on day 3 and replaced on day 6 after seeding. The cells were used on day 7. Expression of the CD11c marker was assessed by flow cytometry to confirm differentiation.

Parasite lysates and protein quantification. *T. gondii* whole lysates were prepared from 2×10^9 to 5×10^9 freshly isolated RH WT tachyzoites. The parasites were resuspended in ice-cold phosphate-buffered saline (PBS) and subjected to three 5-min freeze-thaw cycles, going from liquid nitrogen (LN_2) to a 37°C water bath. The parasites were then sonicated on ice for 10 min, with 1-s pulses at 30% duty cycle. The lysates were centrifuged at 100,000 × *g* for 30 min at 4°C using a fixed-angle TLA-100.3 rotor (Beckman Coulter, Brea, CA), and the high-speed supernatant (HSS) was collected. The protein concentration in the HSS was determined by a bicinchoninic acid (BCA) assay (Pierce, Rockford, IL),

according to the manufacturer's specifications, and adjusted to 2.5 mg/ml, and the HSS was stored at −80°C.

***In vitro* infection for invariant-chain (CD74) induction.** Day 7 BMMϕ were plated at 3×10^5 cells per well in 24-well plates and incubated overnight (ON) to allow adherence. On the following day, the adherent cells were inoculated with freshly harvested *T. gondii* tachyzoites at a multiplicity of infection (MOI) of 3:1. When required, parasites were stained with CellTracker Green CMFDA or CellTrace Far Red DDAO-SE (Molecular Probes, Carlsbad, CA) at 20 μM in DMEM for 30 min at room temperature before inoculating the BMMϕ. After inoculation, the cells were incubated for 4 h, the extracellular parasites were rinsed away, and fresh medium was added with or without IFN-γ at a final concentration of 100 U/ml (BioSource, Carlsbad, CA). The cultures were incubated for 20 h or the indicated times.

Antigen presentation assay. Day 7 BMDCs were plated at 3×10^5 cells per well in 24-well plates. The cells were then inoculated with freshly harvested *T. gondii* tachyzoites at an MOI of 3:1 for live parasites (RHΔΔ *ptub* RFP, RHΔ*cpsII ptub* Eα-RFP, and RHΔ*cpsII ptub* P30-Eα-RFP) or 8:1 for heat-killed parasites (RHΔ*cpsII ptub* Eα-RFP). After 4 h of incubation, fresh medium was added, and the cells were pulsed or not with Eα peptide (ASFEAQGALANIAVDKA) at a concentration of 1, 5, or 10 μg/ml. The cells were incubated for 18 to 20 h and then harvested for flow cytometry analysis.

Flow cytometry and cell sorting. CD74 and MHC-II expression in BMMϕ was assessed by flow cytometry using a BD FACSAria (BD Biosciences, San Jose, CA). First, Fc receptors were blocked by adding rat IgG and rat anti-mouse CD16/32 (Fcγ III/II; clone 2.4G2; BD Biosciences) in fluorescence-activated cell sorter (FACS) buffer (0.1% bovine serum albumin fraction V [BSA] in PBS) for 15 min on ice. After blocking, the cells were stained with fluorescein isothiocyanate (FITC)-conjugated rat anti-mouse CD74 (clone In-1) and phycoerythrin (PE)-conjugated rat anti-mouse MHC-II (IA/IE) (eBioscience, San Diego, CA) for 30 min. For intracellular staining, cells were first fixed in 1% paraformaldehyde (PFA) for 10 min on ice, the fixative agent was quenched with 0.1 M glycine PBS, and the cells were resuspended in permeabilization buffer (0.05% saponin, 0.1% BSA in PBS) for 20 min. After permeabilization, the cells were stained using the above-mentioned antibody. Isotype-matched antibody, rat IgG2b(κ)-FITC, was used as a staining control (eBioscience). After staining and washing, the cells were fixed again in 1% PFA and analyzed by flow cytometry. Presentation of the model antigen Eα in the context of MHC-II molecules by BMDCs was assessed by flow cytometry after staining the cells with a FITC-conjugated anti-Eα52-68 peptide bound to I-A^b (clone YAe) antibody (eBioscience), as previously described (50), and live cells were analyzed. The flow cytometry data were analyzed using FlowJo software (Tree Star, Ashland, OR).

Sorting of BMMϕ cultures was carried out using a BD FACSAria (BD Biosciences). Cultures were infected with RHΔΔ *ptub* P30-YFP tachyzoites at an MOI of 4:1 for 4 h, after which the extracellular parasites were washed away and fresh medium was added with or without 100 U/ml IFN-γ. The cells were incubated for 20 h, harvested, and stained with 50 μg/ml propidium iodide (PI) (EMD Chemicals, Gibbstown, NJ) prior to sorting; fluorescent cells labeled with PI were considered dead and excluded. The live cells were then gated according to the infection state, where YFP-positive cells were infected and YFP-negative cells were not, and collected separately. The sorted samples were aliquoted and stored at −80°C.

***In vivo* infection and cell analysis.** Four- to 6-week-old WT C57BL/6 mice were infected with 10^6 RHΔΔ *ptub*-RFP tachyzoites intraperitoneally (i.p.). Mesenteric lymph nodes (MLN) of infected animals were harvested 5 days p.i., filtered through 70-μm-pore-size nylon mesh cell strainers (BD Biosciences), and stained for flow cytometry. The staining protocol was performed as described above using the following antibodies: peridinin chlorophyll protein (PerCP)-Cy5.5-conjugated rat anti-mouse CD11b (M1/70), PE-Cy7-conjugated Armenian hamster anti-mouse CD11c (N418), and FITC-rat anti-mouse CD74 (In-1) or FITC-rat anti-mouse MHC-II (IA/IE). Isotype-matched controls were prepared in parallel [rat IgG2b(κ)-FITC and IgG2b(κ)-PerCP-Cy5.5 and Armenian hamster IgG-PE-Cy7].

T cell analysis was performed on cells collected from acutely infected 4- to 6-week old WT, CD74$^{-/-}$, H2-DM$^{-/-}$, and dKO mice. Briefly, the mice were infected i.p. with 10^3 PruΔ tachyzoites. After 8 days, MLN were collected, filtered through 70-μm-pore-size cell strainers, and stained for flow cytometry using the following antibodies: FITC-Armenian hamster anti-mouse CD3ε (145-2C11), PE-rat anti-mouse CD4 (L3T4), allophycocyanin (APC)-rat anti-mouse CD25 (PC61.5), PE-Cy7-rat anti-mouse CD44 (IM7), and APC-eFluor780-rat anti-mouse CD62L (MEL-14) (eBioscience). Isotype-matched controls were prepared in parallel [Armenian hamster IgG-FITC, rat IgG2b(κ)-PE and IgG2b(κ)-PE-Cy7, rat IgG1(λ)-APC, and rat Ig2a(κ)-APC-eFluor780]. Sera from these acutely infected mice and control uninfected mice were collected. IFN-γ levels were measured by enzyme-linked immunosorbent assay (ELISA) using the eBioscience Mouse IFN-γ ELISA Ready-SETGo! kit according to the manufacturer's specifications.

For chronic infections, 10^3 PruΔ tachyzoites were injected i.p. For real-time (RT)-PCR analysis of the brain cyst burden, brains were collected 20 days p.i.

Histology. Brains from WT, CD74$^{-/-}$, H2-DM$^{-/-}$, and dKO mice 10, 15, 20, and 25 days after infection with 10^3 PruΔ tachyzoites i.p. were collected and fixed in neutral buffered formalin (10% [vol/vol]). Brains from uninfected control animals were collected, as well. Processing and staining of brain tissue for histology were carried out by Histopathology Services at Charles River. After fixation, 3 or 4 cross sections were taken through the cerebrum and one representative section through the cerebellum. The sections were embedded in paraffin, placed onto glass microscopy slides, and stained with hematoxylin and eosin. Photographs were taken using a Nikon Eclipse E800 microscope equipped with a Nikon DXM1200F digital camera and Nikon ACT-1 software.

Immunofluorescence and colocalization microscopy. Day 7 BMMϕ cultures (5×10^4 cells) were plated on glass coverslips in 24-well plates and incubated ON at 37°C and 5% CO_2 to allow the cells to firmly adhere to the coverslips. The following day, the cells were infected with freshly lysed out *T. gondii* RH WT tachyzoites at an MOI of 2:1. Alternatively, cells were inoculated with heat-killed (HK) (at 56°C for 10 min prior to inoculation) parasites at an MOI of 10:1, treated with *T. gondii* lysates at a concentration of 200 μg/ml, infected with *Leishmania donovani* promastigotes (a kind gift from Armando Jardim, Institute of Parasitology, Sainte-Anne-de-Bellevue, Canada) at an MOI of 15:1 or infected with *Salmonella enterica* serovar Typhimurium 14028 bacteria (a kind gift from Hervé Le Moual, McGill University, Montreal, Canada) at an MOI of 20:1 in the absence of antibiotics. After 4 h, the extracellular parasites were rinsed away, and fresh medium was added with or without 100 U/ml IFN-γ. The cells were fixed after 20 to 24 h or at the indicated times with 3.7% PFA in PBS for 10 min at room temperature. Following fixation, the coverslips were washed extensively with PBS, and the cells were permeabilized with 0.2% Triton X-100 in PBS for 5 min and blocked with 10 mg/ml BSA, 10% FBS in PBS with mouse IgG (Sigma) for 15 min. Primary antibodies were incubated for 1 h at room temperature: rat anti-mouse CD74 (clone In-1), rat anti-mouse IA/IE (MHC-II) (eBioscience), polyclonal rabbit anti-mouse Giantin (Golgi apparatus), polyclonal rabbit anti-mouse GRP78 BiP (ER), polyclonal rabbit anti-mouse EEA-1 (early endosomes [EE]), polyclonal rabbit anti-mouse LC3A/B (autophagosomes) (Abcam, Cambridge, MA), and polyclonal goat anti-mouse CD63 (M-13) (lysosomes) (Santa Cruz Biotechnology, Santa Cruz, CA). Fluorophore-conjugated secondary antibodies were incubated for 1 h at room temperature: donkey anti-rat IgG(H+L) Alexa Fluor 488 and goat anti-rabbit IgG(H+L) Alexa Fluor 488 or 594 (Invitrogen, Carlsbad, CA). To stain the DNA and visualize the nuclei, samples were stained with 4′,6-diamidino-2-phenylindole dilactate (DAPI). Coverslips were mounted onto microscope slides with Fluoromount G (Southern Biotech, Birmingham, AL). Samples were visualized using a Nikon (Tokyo, Japan) Eclipse

TE2000-U microscope, and images were deconvolved using AutoQuant X software (Media Cybermetrics, Phoenix, AZ) and processed with Adobe Photoshop (San Jose, CA). For colocalization experiments, a Zeiss LSM710 confocal microscope with Zen2010 software (Zeiss Canada, Toronto, Canada) was used to acquire images, and image processing and statistical calculations were performed with Fiji (51).

Western blotting. Cells and extracellular tachyzoites were resuspended in lysis buffer (1% Triton X-100, 10 mM Tris, 150 mM NaCl) supplemented with protease inhibitor cocktail (Sigma-Aldrich) and DNase I (1 μg/ml). Protein material was precipitated ON in a methanol-ethanol-acetone (2:1:1) mixture at −80°C. After precipitation, the protein material was resuspended in SDS-PAGE loading buffer containing beta-mercaptoethanol, boiled for 5 min, and loaded onto a precast 4 to 20% Tris-HCl minigel (Bio-Rad, Hercules, CA). Protein material equivalent to 2×10^6 and 10^8 extracellular parasites was loaded per lane. The gels were run at 20 V using a Tetracell apparatus (Bio-Rad) and then transferred to nitrocellulose membranes. The membranes were blocked in 5% dry skim milk in TTBS (15 mM Tris-HCl, 140 mM NaCl, 0.05% Tween 20) ON at 4°C. The membranes were probed with monoclonal rat anti-mouse CD74 clone In-1 (BD Pharmingen, San Jose, CA), followed by a goat-anti-rat IgG(H+L) antibody conjugated to horseradish peroxidase (HRP) (Santa Cruz Biotechnology, Santa Cruz, CA). Bands were revealed using SuperSignal West Femto substrate or ECL West blotting substrate (Pierce) according to the manufacturer's specifications. Loading control was performed by probing with a rabbit anti-cytoskeletal actin antibody (Bethyl Laboratories, Montgomery, TX), followed by a goat-anti-rabbit IgG(H+L) antibody conjugated to HRP (Bio-Rad), and the presence of parasites was verified by probing with mouse anti-GRA3 antibody, followed by a goat-anti-mouse IgG(H+L) antibody conjugated to HRP (Bio-Rad).

Reverse transcription and RT-PCR. RT-PCR was performed using the Power SYBR green Cells-to-Ct kit (Applied Biosystems, Carlsbad, CA) according to the manufacturer's instructions. Briefly, 10^5 sorted BMMϕ were lysed with the lysis solution provided with the kit, followed by reverse transcription using the Bio-Rad DNA Engine (Peltier Thermal Cycler) and the 20× reverse transcription enzyme mix with 2× SYBR reverse transcription buffer. The concentration of the synthesized cDNA was estimated by absorbance at 260 nm using a NanoDrop (Wilmington, DE) ND-1000. PCRs were performed in a 7500 real-time PCR system (Applied Biosystems) using the Power SYBR green PCR master mix, 400 nM (final concentration) each designed PCR primer (19 to 25 nucleotides) (see Table S2 in the supplemental material), and 3 μg of cDNA in a total volume of 20 μl. The β-actin primer provided in the SYBR green Cells-to-Ct control kit was used to amplify the endogenous control gene for normalization of the transcripts. The mRNA transcription level analysis was assessed using the $2^{-\Delta\Delta Ct}$ method (52) using the uninfected and unstimulated BMMϕ sample as a reference.

Genomic DNA isolation and quantification of the parasite burden by RT-PCR. Genomic DNA (gDNA) was isolated from MLN of acutely infected mice or brains of chronically infected animals using a Roche High Pure PCR template preparation kit according to the manufacturer's specifications. To measure acute parasitemia or the cyst burden, the 35-fold repetitive *T. gondii* B1 gene (53) was amplified by real-time PCR using Power SYBR green PCR master mix (Applied Biosystems) with the $MgCl_2$ concentration adjusted to 3.5 μM in a 50-μl reaction volume, 0.5 μg of template gDNA, and 0.5 μM each forward primer (5′-TCCCCTCTGCT GGCGAAAAGT-3′) and reverse primer (5′-AGCGTTCGTGGTCAACT ATCGATTG-3′) (Integrated DNA Technologies, Coralville, IA) (54). The B1 gene was amplified using an ABI 7500 RT-PCR system with 10 min of initial denaturation at 95°C, followed by 35 cycles of 15 s of denaturation at 95°C, 30 s of annealing at 52°C, and 30 s of extension at 72°C. The threshold value was defined as 30 times the standard deviation (SD) of the baseline fluorescent signal, and cycle threshold (C_T) values were acquired during the annealing step. The C_T values were normalized using the mouse β-actin gene under the same conditions outlined above in separate tubes, but with 0.2 μM each forward (5′-CACCCACACTGTGCCCATCTACGA-3′) and reverse (5′-CAGCGGAACCGCTCATTGCCAATGG-3′) primer (55) and 2.5 μM $MgCl_2$.

RESULTS

***T. gondii* infection inhibits transcription of MHC-II (H2) and H2-DM genes but induces transcription of CD74 and expression of p41 and p31 protein isoforms.** We assessed the transcriptional profiles of different MHC-II-related genes, MHC-II, CD74, and H2-DM in *T. gondii*-infected cells. BMMϕ cultures were infected for 4 h with a transgenic parasite line secreting YFP in the PV, either stimulated with 100 U/ml IFN-γ or left unstimulated for 20 h, and sorted by means of FACS according to their infection status. RT-PCR analyses on sorted cells revealed that transcription of both p41 and p31 CD74 isoforms was induced in infected cells in the absence of IFN-γ stimulation, but not that of other MHC-II (H2-Aα, H2-Aβ1, and H2-Eβ1) and H2-DM (H2-DMα, H2-DMβ1/2) genes, suggesting uncoordinated expression of these genes (Fig. 1A). On the other hand, IFN-γ-induced transcription of the genes, including both CD74 isoforms, was inhibited in infected cells, in agreement with previous reports showing inhibition of IFN-γ-mediated transcription by *T. gondii* (15, 22, 33, 34).

Both p41 and p31 CD74 protein isoforms were detected in infected cells (Fig. 1B), whether stimulated or not, while they were detected only in uninfected IFN-γ-primed cells. These observations mirrored the transcriptional profiles measured by RT-PCR. Interestingly, Western blot analysis revealed different patterns of li processing: a p10 proteolytic product (or small leupeptin-induced invariant chain [sLIP]) was detected in uninfected IFN-γ-stimulated BMMϕ, but it was moderately more abundant in the *T. gondii*-infected cells, both unstimulated and IFN-γ stimulated, which could suggest a slight bias in CD74 processing.

CD74 molecules accumulate mostly in the ER of cells infected with live *T. gondii* until egress of the parasite, even in the absence of IFN-γ stimulation. CD74 expression was significantly induced in BMMϕ infected with *T. gondii* tachyzoites in the absence of IFN-γ stimulation (Fig. 2); CD74 molecules were detectable approximately 16 h after parasite inoculation and accumulated until parasite egress, as observed by fluorescence microscopy (see Fig. S1 in the supplemental material). CD74 accumulation was not observed in uninfected bystander cells, suggesting that this induction was cell autonomous and occurred only within infected cells. Furthermore, cells that had phagocytosed HK parasites or had been treated with parasite lysates failed to increase CD74 levels (Fig. 2). These observations indicate that active host cell invasion by live parasites is required to induce this phenotype. The induction of CD74 expression was not observed when macrophages were infected with other intracellular pathogens, namely, *S. enterica* serovar Typhimurium and *L. donovani* (Fig. 2B and C), both known to inhibit MHC-II expression (56–58).

Colocalization experiments revealed that the accumulation of CD74 molecules occurred predominantly in the ER of *T.* gondii-infected BMMϕ (Fig. 3A), although li molecules were also detected to some extent in the Golgi apparatus and to a much lower degree in EE (Fig. 3B and C). Colocalization of CD74 was not observed in the $LC3^+$ (autophagosome) or in the $CD63^+$ (lysosome) compartment (see Fig. S2A and B in the supplemental material). These observations suggest that the majority of CD74 molecules are withheld in early endocytic compartments and do not efficiently traffic to more mature endocytic compartments.

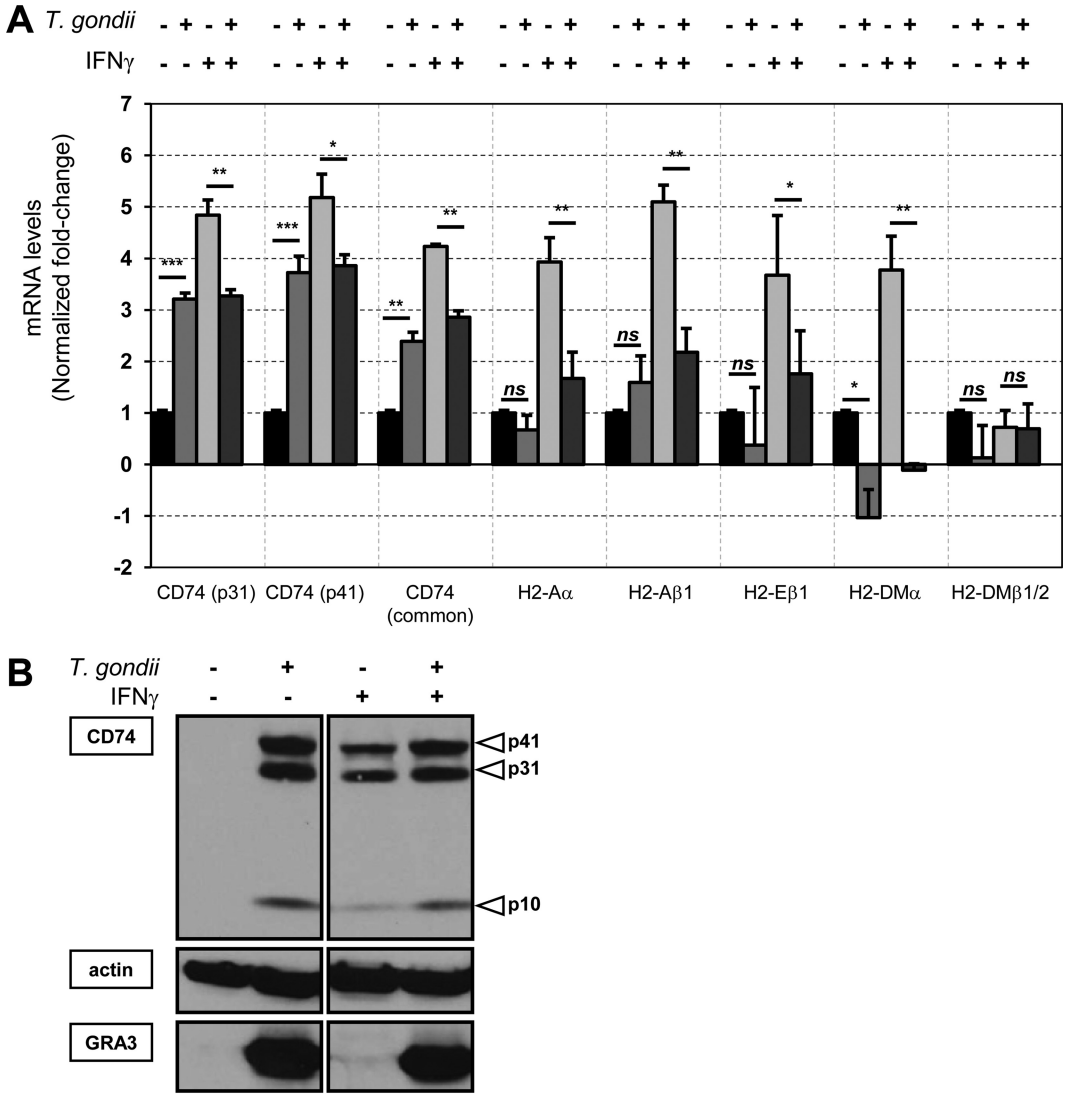

FIG 1 *T. gondii* infection inhibits transcription of MHC-II and H2-DM genes but induces transcription of CD74 and expression of p41 and p31 protein isoforms in the absence of IFN-γ. (A) RT-PCR analysis was performed on BMMϕ cultures inoculated with YFP-expressing *T. gondii* (MOI = 3:1), left unstimulated or stimulated with 100 U/ml IFN-γ ON, and sorted by FACS according to infection status. The data were calculated using the $2^{-\Delta\Delta Ct}$ method (52), where the uninfected, unstimulated cells were used to calculate the normalized fold change. The error bars indicate SD between biological replicates from one representative experiment out of three independent experiments. Significance was calculated using Student's *t* test (*ns*, not significant; *, $P < 0.05$; **, $P < 0.01$; ***, $P < 0.001$). (B) Expression of p41 and p31 CD74 isoforms and the levels of the p10 proteolysis product in BMMϕ cultures were assessed by Western blotting. Briefly, cultures were inoculated with YFP-expressing *T. gondii* (MOI = 3:1), left unstimulated or stimulated with 100 U/ml IFN-γ ON, and sorted by FACS according to infection status. The material from 10^6 BMMϕ was loaded in the indicated lanes of 4 to 20% Tris-HCl SDS-PAGE gels. Actin was probed as a loading control, and probing for GRA3 confirmed the presence of parasites within infected cells.

As previously stated, CD74 can traffic from the ER to the plasma membrane through AP2-dependent sorting (30, 31). At the cell surface, CD74 can act as a receptor for the proinflammatory cytokine macrophage migration inhibitory factor (MIF) (59). Therefore, we used differential staining techniques, which allowed us either to stain surface molecules only or to stain both surface and intracellular molecules by permeabilizing the cell membrane, for flow cytometry to determine if CD74 also accumulated at the surfaces of *T. gondii*-infected cells. When BMMϕ were stained for surface CD74 molecules (i.e., without permeabilization of the cell membrane), no major differences in surface CD74 expression were measured between uninfected and *T. gondii*-infected cells; however, following fixation and permeabilization with saponin, a marked increase of CD74 levels was detected in infected cells in the absence of exogenous IFN-γ (Fig. 4A). Also, potential endogenous secretion of TNF-α or type I IFNs (IFN-α and IFN-β), cytokines known to induce CD74 expression (60–62), did not play a role in the phenotype, since BMMϕ from TNF-α and type I IFN receptor (IFN-AR1) KO mice infected with *T. gondii* also displayed enhanced levels of CD74 (see Fig. S3 in the supplemental material).

The higher CD74 expression levels observed in *Toxoplasma*-infected cells did not correlate with higher MHC-II expression levels (Fig. 4B). IFN-γ stimulation did not lead to increased levels of CD74 or MHC-II in infected cells, as seen in uninfected control cells, in which expression upregulation was coordinated, as ex-

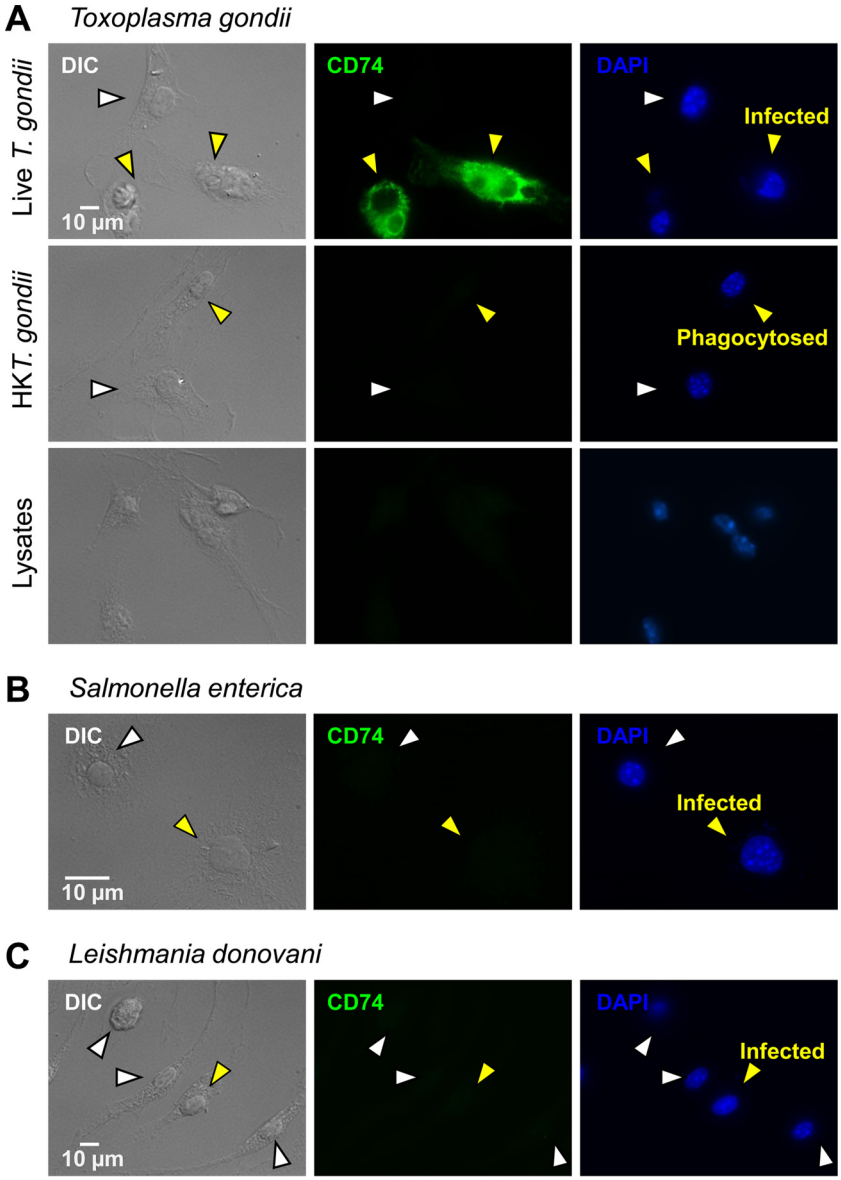

FIG 2 *T. gondii*, but not other intracellular pathogens, upregulates CD74 protein expression in infected BMMϕ. BMMϕ cultures were infected with *T. gondii* RH WT tachyzoites (MOI = 2:1), inoculated with heat-killed (HK) parasites (MOI = 10:1), and treated with 200 μg/ml of parasite lysates (A); infected with *S. enterica* serovar Typhimurium bacteria (MOI = 20:1) (B); or infected with *L. donovani* promastigotes (MOI = 15:1) (C). After 4 h, the extracellular pathogens were rinsed away, fresh medium was added (antibiotics were resupplemented in wells inoculated with bacteria), and the cells were incubated for 20 h and fixed with 3.7% PFA in PBS. The cells were stained for CD74 (green) and with DAPI. Samples were visualized by epifluorescence microscopy, and the images were deconvolved using AutoQuant X software. CD74 expression levels are shown in uninfected cells (white arrowheads) and infected cells or cells containing phagocytosed parasites (yellow arrowheads). The fields are representative of entire cultures and of the results of three independent experiments. DIC, transmitted-light differential interference contrast.

pected. These observations corroborate the uncoordinated expression patterns between CD74 and MHC-II seen at the transcriptional level in *T. gondii*-infected cells (Fig. 1A).

Accumulation of CD74 is triggered by both virulent type I and avirulent type II strains, does not require parasite replication, and occurs *in vivo*. Significant differences have been demonstrated between type I (virulent) and type II (avirulent) strains of *T. gondii* in the modulation of immune responses and signaling pathways (17, 18, 63). The induction of CD74 was not found to be strain specific and was observed in BMMϕ infected with either the virulent type I RH or the avirulent type II Pru strain (Fig. 5A). Active parasite replication was not required, since a nonreplicating, uracil-deprived Δ*cpsII* strain (i.e., a uracil-auxotroph strain [44]) also induced CD74 in infected cells (Fig. 5B). This observation also helped rule out the possibility that the phenotype seen in infected cultures was caused by exposure to material from lysed-out infected cells, since the uracil-deprived mutant did not egress.

To validate the relevance of the accumulation of CD74 in *T. gondii*-infected cells *in vivo*, CD74 expression was analyzed in $CD11b^+$ (panmacrophage marker) and $CD11c^+$ $CD8\alpha^-$ (myeloid dendritic cells) cells from MLN of WT C57BL/6 mice infected with virulent type I RH *T. gondii* tachyzoites. Parasites ex-

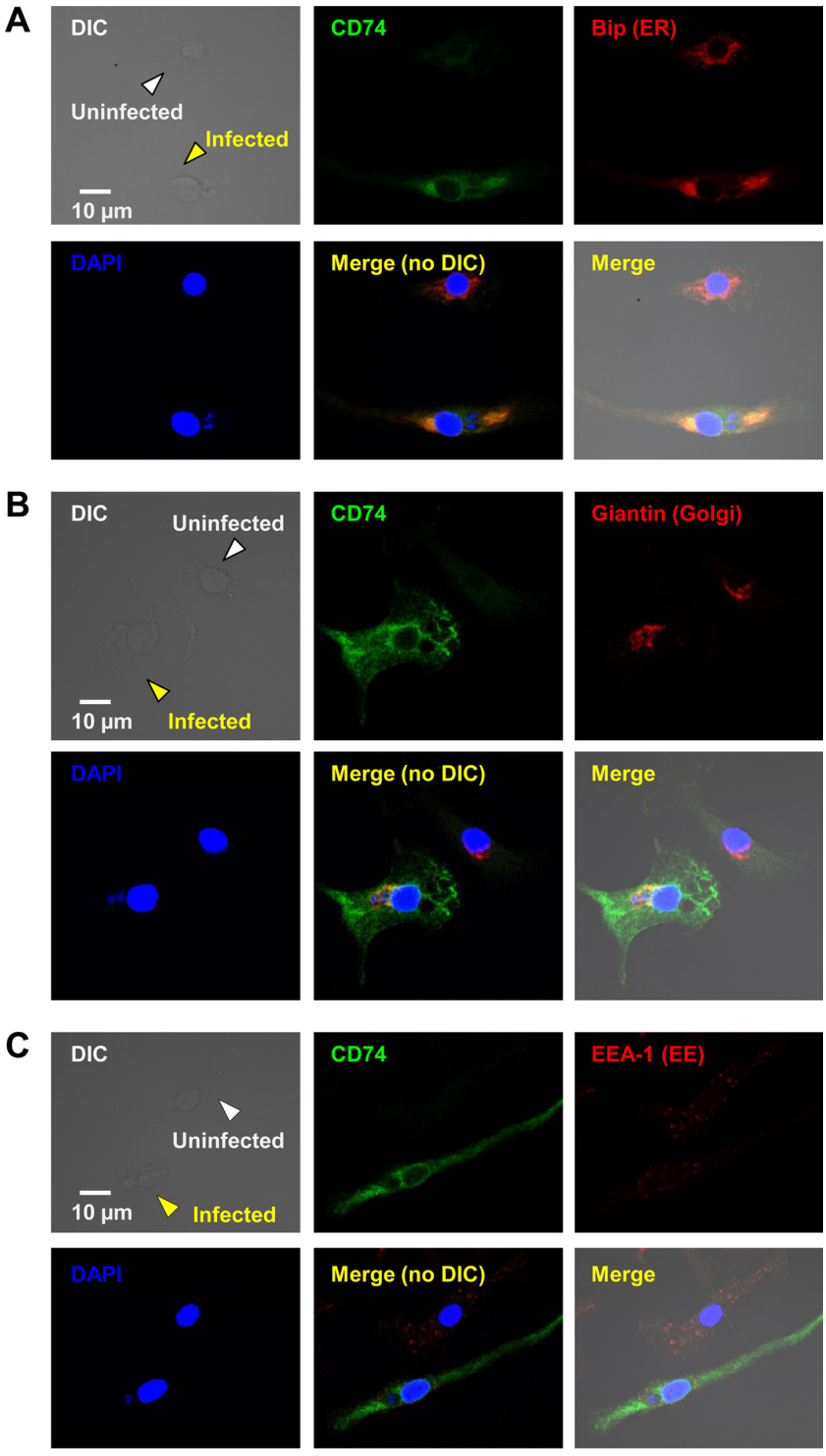

FIG 3 CD74 accumulates mostly in the ER, but also in the Golgi apparatus and EE, in unstimulated, infected BMMϕ. Colocalization experiments for CD74 (green) were carried out with different markers for the ER (Bip) (A), the Golgi apparatus (Giantin) (B), and early endosomes (EEA-1) (C) (all red) in *T. gondii*-infected BMMϕ cultures (MOI = 2:1) left unstimulated. Z-stacks were acquired by confocal microscopy, followed by image processing, merging, and statistical calculations. Uninfected (white arrowheads) and infected (yellow arrowheads) cells are shown within the same fields. (A) Through statistical analyses, a colocalization coefficient (R_{coloc}, where 1 is total colocalization and 0 no colocalization) of 0.73 and a threshold split Mander's coefficient (tM, where the total pixel intensity was normalized to avoid issues with absolute intensities) of 0.74 were obtained, suggesting significant colocalization of CD74 in the ER. (B and C) CD74 molecules were also found in the Golgi apparatus (R_{coloc} = 0.41; tM = 0.37) (B) and EE (R_{coloc} = 0.32; tM = 0.47) (C) to a much lesser extent. These fields are representative of entire cultures and of the results of three independent experiments.

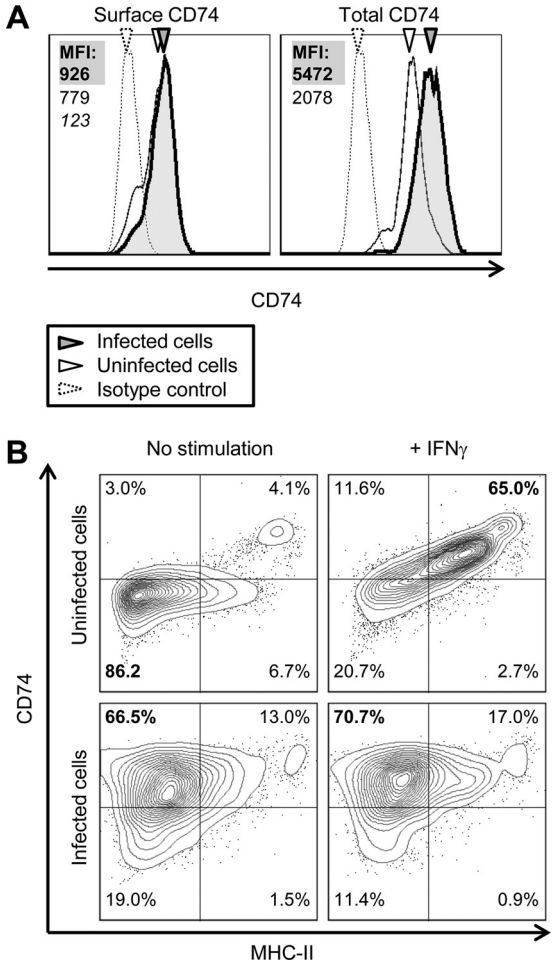

FIG 4 The accumulation of CD74 occurs predominantly intracellularly, with low expression at the cell surface, while MHC-II levels remain low. (A) BMMϕ cultures were left uninfected (white arrowheads) or were inoculated with CellTrace Far Red DDAO-stained parasites (MOI = 3:1) (gray arrowheads). The cells were stained with a FITC-labeled anti-CD74 antibody either after fixation with 1% PFA or after permeabilization with 0.05% saponin, staining surface and intracellular molecules, and then analyzed by flow cytometry. The level of staining is reported as the mean fluorescence intensity (MFI) value, as indicated for each population (italicized for the isotype control, lightface for uninfected control cells, and boldface for infected cells). (B) BMMϕ cultures were left uninfected (top) or were infected with fluorescent parasites (MOI = 3:1) (bottom). After 4 h, fresh medium was added with (right) or without (left) 100 U/ml IFN-γ, and the cultures were incubated for 20 h. The cells were stained for CD74 and MHC-II after permeabilization and then analyzed by flow cytometry. The bottom diagrams display expression patterns of infected cells only, following a gating strategy that identified cells containing fluorescent parasites.

pressing RFP were used to infect mice i.p. in order to distinguish infected cells from uninfected cells by flow cytometry. Similarly to *in vitro* observations, infected macrophages and myeloid DCs from infected mice expressed higher levels of CD74 than uninfected cells, while MHC-II levels remained at relatively similar levels (Fig. 5C).

Accumulation of CD74 and reduced expression of H2-DM inhibit presentation of endogenous parasite-derived antigens in the context of MHC-II. To assess the impacts of invariant-chain accumulation and inhibition of H2-DM on MHC-II antigen presentation, we first used the Eα model antigen and YAe antibody system to measure functional MHC-II antigen presentation by pAPCs *in vitro* (45, 46, 50). The YAe antibody binds specifically to MHC-II I-A^b molecules ($H2^b$ haplotype, i.e., C57BL/6 mice) loaded with the I-Eα peptide (from the $H2^d$ haplotype, i.e., BALB/c mice) without binding to other MHC-II molecules loaded with irrelevant antigens, thus allowing the measurement of antigen-specific presentation (Fig. 6A). The ability of BMDCs from $CD74^{-/-}$ and H2-$DM^{-/-}$ mice to present exogenous Eα peptide was markedly impaired, while their WT counterparts efficiently presented the antigen on MHC-II molecules (Fig. 6B). WT and H2-$DM^{-/-}$ BMDCs infected with live parasites expressing Eα in their cytosol or secreting the antigen in the PV presented the parasite-derived antigen at low levels, an observation in agreement with previous reports on the ability of *T. gondii* to inhibit antigen presentation by the infected host cell (22–24). In stark contrast, *T. gondii*-infected $CD74^{-/-}$ cells efficiently presented the parasite-derived Eα peptide on MHC-II molecules. However, WT, $CD74^{-/-}$, and H2-$DM^{-/-}$ BMDCs efficiently presented the antigen after internalizing (phagocytosing) HK Eα-expressing parasites. Both WT and $CD74^{-/-}$, but not H2-$DM^{-/-}$, BMDCs infected with the control parasites expressing RFP only were still capable of efficiently presenting exogenously derived Eα peptide after infection. Taken collectively, these results indicate that accumulation of CD74 induced by the parasite inhibits MHC-II presentation of parasite-derived or endogenously acquired antigens but does not interfere with MHC-II presentation of exogenous antigens.

Accumulation of CD74 during acute toxoplasmosis affects parasite dissemination, while CD74 and H2-DM differentially impact $CD4^+$ T cell activation and IFN-γ production. Given the phenotype observed with the previous *in vitro* system, we sought to assess the impacts of CD74 and H2-DM on $CD4^+$ T cell priming and activation during acute toxoplasmosis. $CD4^+$ T cells were collected from MLN of acutely infected WT, $CD74^{-/-}$, and H2-$DM^{-/-}$ mice. Flow cytometry analysis revealed a higher proportion of $CD3\varepsilon^+$ $CD4^+$ lymphocytes displaying a $CD25^{hi}$ $CD44^{hi}$ $CD62L^{low}$ activated phenotype in $CD74^{-/-}$ than in WT animals (62.0% $CD62L^{low}$ versus 38.7%, respectively) (Fig. 7A). Infected H2-$DM^{-/-}$ mice, on the other hand, had a lower proportion of $CD4^+$ T cells displaying an activated phenotype (10.3% $CD62L^{low}$). It is important to point out that total $CD3\varepsilon^+$ $CD4^+$ T cell numbers differed between the different mouse strains in both naive and infected animals. ELISA measurements revealed higher levels of IFN-γ in sera of $CD74^{-/-}$ mice than in sera of WT mice and H2-$DM^{-/-}$ mice (Fig. 7B). To examine whether the increased T cell activation and IFN-γ production observed in $CD74^{-/-}$ mice was associated with increased parasite replication, the parasite burden was measured by RT-PCR on MLN from acutely infected mice. Parasite loads were 25 times higher in $CD74^{-/-}$ than in WT and H2-$DM^{-/-}$ mice (Fig. 7C). *In vitro* analysis revealed no differences in intracellular parasite replication rates or in egress between infected WT and $CD74^{-/-}$ BMMϕ (see Fig. S4 in the supplemental material).

Considering the major but functionally distinct roles of CD74 and H2-DM in the MHC-II pathway, we assessed the dual impact of their simultaneous absence on the course of infection. Double-KO mice were generated by breeding $CD74^{-/-}$ and H2-$DM^{-/-}$ single-KO strains and then crossing the heterozygote progeny. The activation profiles of $CD3\varepsilon^+$ $CD4^+$ T cells were higher (75.3% $CD62L^{low}$), but serum IFN-γ levels were compara-

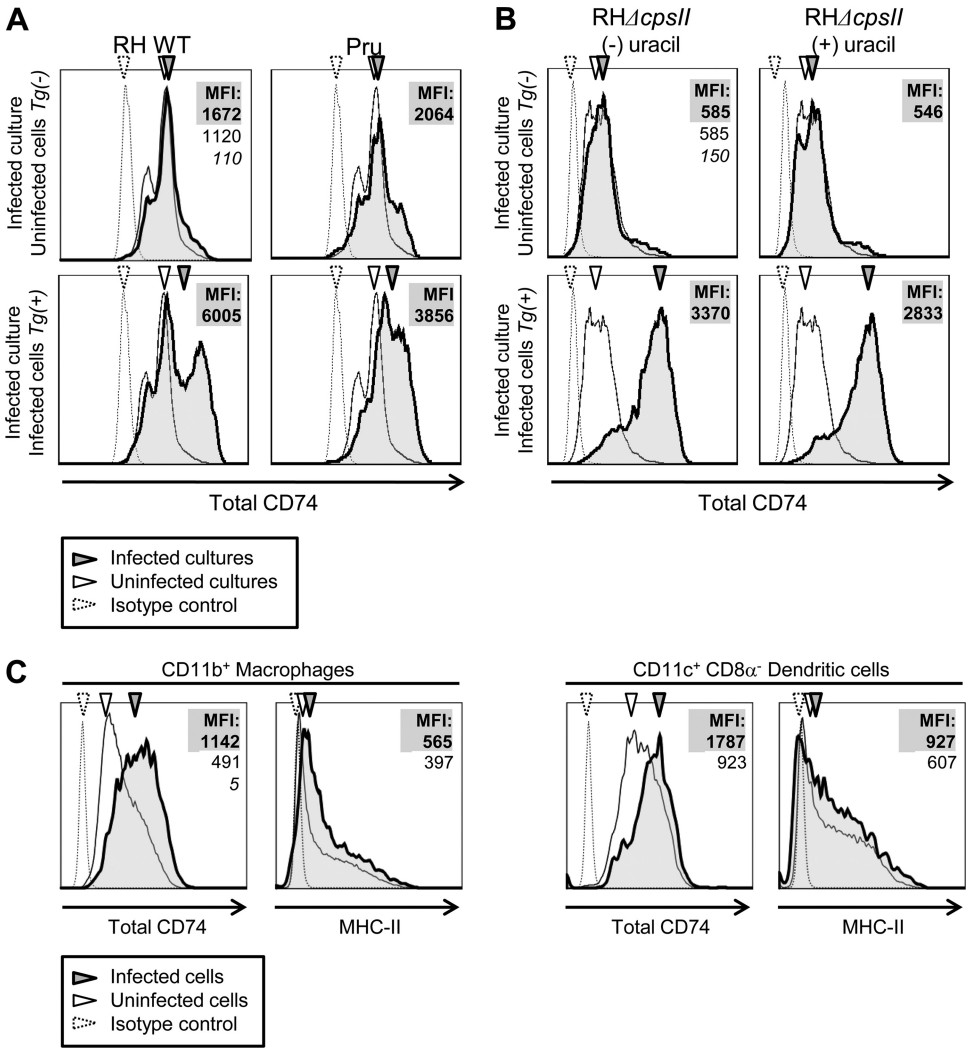

FIG 5 Accumulation of CD74 is triggered by both virulent type I and avirulent type II strains, does not require active parasite replication, and occurs *in* vivo. (A and B) BMMϕ cultures were infected (MOI = 3:1) with type I RH WT or type II Pru tachyzoites (A) or the uracil-auxotroph mutant RHΔ*cpsII* in the absence (left) or presence (right) of exogenous uracil (B) and left unstimulated ON, and the cells were fixed, permeabilized, stained for total CD74 proteins, and analyzed by flow cytometry. CD74 levels and MFI values are indicated. Tg^-, uninfected bystander cells; Tg^+, infected cells. (C) Flow cytometry analysis was performed on cells from the MLN of WT C57BL/6 mice 5 days after i.p. infection with 10^6 RHΔΔ *ptub*-RFP tachyzoites. $CD11b^+$ (macrophages) and $CD11c^+$ $CD8\alpha^-$ (myeloid DCs) cell subsets were identified and stained for CD74 and MHC-II. CD74 expression in infected cells and uninfected cells from the same organ and for the isotype control are shown, as well as the MFI values. Three independent infection trials that included at least three animals were carried out. Shown are representative values for one infected animal.

ble to those of infected WT controls (Fig. 7A and B). Similarly to $CD74^{-/-}$ mice, parasitemia levels in draining lymph nodes were significantly higher in dKO mice than in WT or H2-$DM^{-/-}$ mice (18-fold increase) (Fig. 7C).

Absence of H2-DM leads to a higher brain cyst burden in chronically infected animals, whereas absence of both CD74 and H2-DM is fatal during chronic infection. Although differences in the magnitude of immune responses were measured in single-KO and dKO mice at the acute phase of infection, all the mutant mice survived acute infection. However, brain cyst burdens varied significantly in these mice (Fig. 8A). Quantitative-RT-PCR analysis revealed a 6-fold increase in brain cyst burdens in H2-$DM^{-/-}$ mice compared to WT controls. While no significant differences were observed between WT and $CD74^{-/-}$ mice, cyst burdens in dKO mice increased 30-fold, and histological sections of the infected brains confirmed these observations (Fig. 8B). Isolated cysts were spotted in the brains of WT and $CD74^{-/-}$ mice, while large clusters of cysts were seen in H2-$DM^{-/-}$ and dKO mice. All dKO mice succumbed during the early chronic phase of infection, even when infected with a nonlethal dose of the type II strain (Fig. 8C).

DISCUSSION

IFN-γ is the major effector molecule controlling *T. gondii* infection, and its production occurs within 3 days after initial infection (7–9). The fact that the parasite subverts many functions of the immune system allows the establishment of a chronic infection. In the present study, we provide evidence of enhanced transcription and protein synthesis of the MHC-II-associated invariant chain (CD74) in infected cells in the absence of IFN-γ *in vitro*. Although

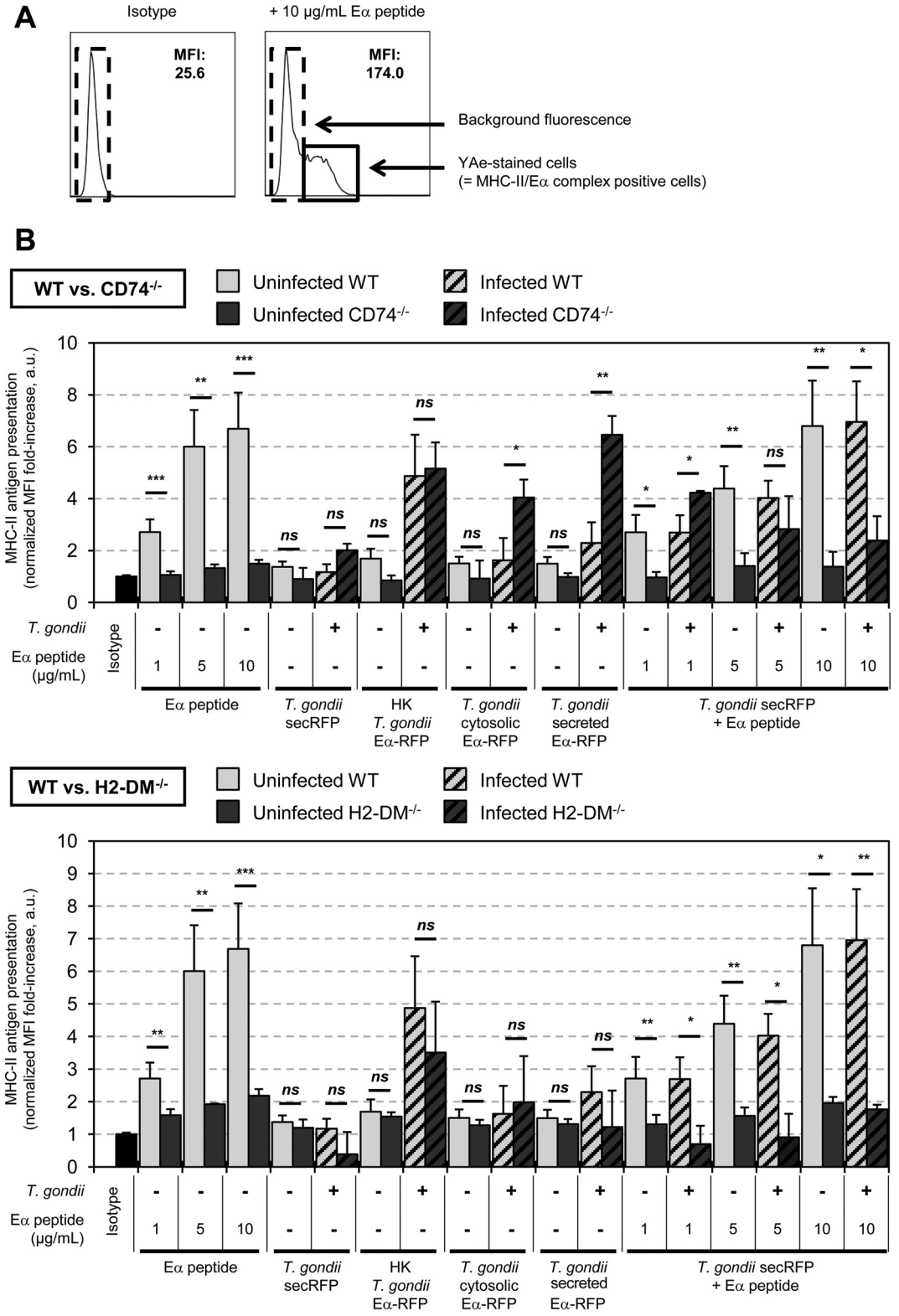

FIG 6 The accumulation of CD74 in infected BMDCs and reduced expression of H2-DM inhibit presentation of endogenously acquired, parasite-derived antigens in the context of MHC-II. BMDC cultures (WT, CD74$^{-/-}$, and H2-DM$^{-/-}$) were inoculated with either *T. gondii* tachyzoites at an MOI of 3:1 for live parasites (RHΔΔ *ptub* RFP, RHΔ*cpsII ptub* Eα-RFP, and RHΔ*cpsII* ptub P30-Eα-RFP) or 8:1 for HK parasites (RHΔ*cpsII ptub* Eα-RFP). After 4 h of incubation, fresh medium was added and pulsed or not with Eα peptide at concentrations of 1, 5, and 10 μg/ml. The cells were incubated ON and then harvested and stained for flow cytometry analysis. (A) Representative flow cytometry histograms and MFI values indicating background fluorescence (dashed boxes) and positive YAe staining (i.e., MHC-II/Eα complex-positive sample), as determined for the isotype control (left) and a positive sample (right). (B) MFI values were calculated using the FlowJo analysis software and were normalized to the MFI value obtained for the isotype control, which determined the normal background fluorescence. The data are expressed as the fold increase compared to background fluorescence in arbitrary units (a.u.), where a value of 1 is no Eα antigen presentation. For cultures inoculated with parasites, infected cells or those that had phagocytosed HK parasites were distinguished from uninfected bystander cells by gating according to RFP fluorescence. SD values, indicated by the error bars, were calculated from the results of four independent experiments. Significance was calculated using Student's *t* test (*ns*, not significant; *, $P < 0.05$; **, $P < 0.01$; ***, $P < 0.001$); values for WT cultures were used as a reference for each condition.

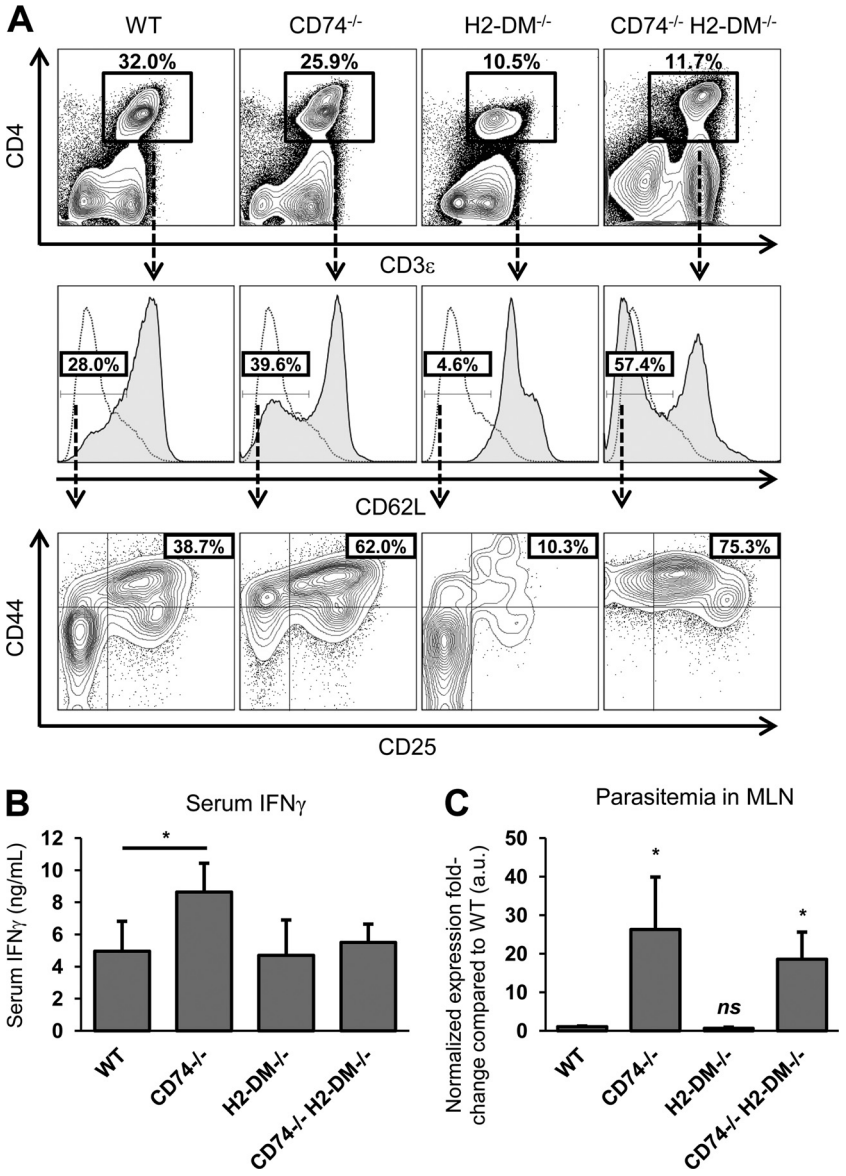

FIG 7 Accumulation of CD74 during acute toxoplasmosis affects parasite dissemination, while CD74 and H2-DM differentially impact $CD4^+$ T cell activation and IFN-γ production. (A) Flow cytometry analysis of $CD4^+$ T cells collected from MLN of acutely infected WT, $CD74^{-/-}$, $H2\text{-}DM^{-/-}$, and dKO ($CD74^{-/-}$ $H2\text{-}DM^{-/-}$) mice was carried out. $CD3\varepsilon^+$ $CD4^+$ positive cells were gated (top) and separated according to high or low CD62L expression (middle; the expression pattern is shown by the shaded curves). Determination of $CD62L^{low}$ populations was accomplished by gating according to the isotype control (unshaded curves). Gating according to CD25 and CD44 expression was performed (bottom), and values (percentages) for the proportions of cells included within the $CD62L^{low}$ and $CD25^{high}$ $CD44^{high}$ gates are indicated. Three independent infection trials, which included at least three animals, were carried out. Shown are representative values from one infected animal. (B) IFN-γ levels in sera from acutely infected mice were measured by ELISA with an eBioscience Mouse IFN-gamma ELISA Ready-SET-Go! kit. The error bars indicate SD calculated from values obtained from three infected mice (for each strain). (C) RT-PCR was performed on gDNA purified from MLN of acutely infected mice. The *T. gondii* B1 gene was amplified to measure the parasite load. C_T values were normalized using the mouse β-actin gene, and the $2^{-\Delta\Delta Ct}$ method was used to calculate the fold increase, where the reference values were those for the infected WT mice. The error bars indicate SD calculated from values obtained from three infected mice (for each strain). Significance was calculated using Student's *t* test (*ns*, not significant; *, $P < 0.05$).

MHC-II, H2-DM, and CD74 gene transcription and protein expression are typically coordinated (64), active invasion by *T. gondii* leads to uncoordinated expression of these components in infected professional antigen-presenting cells. At a genomic level, the murine CD74 promoter consists of promoter and enhancer elements, both unique to CD74 and shared with other class II genes (65), which could explain the differential mRNA expression between MHC-II genes and the CD74 gene in infected cells. *T. gondii* infection may trigger a transcriptional cascade that affects DNA elements unique to CD74 while actively suppressing additional IFN-γ-induced gene transcription. This phenotype was not observed in cells infected with other intracellular pathogens known to inhibit MHC-II expression, namely, *L. donovani* (56, 57) and *S. enterica* serovar Typhimurium (58), which suggests modulation of the MHC-II pathway specific to *T. gondii*. Induction of CD74 required active invasion by parasites, since CD74

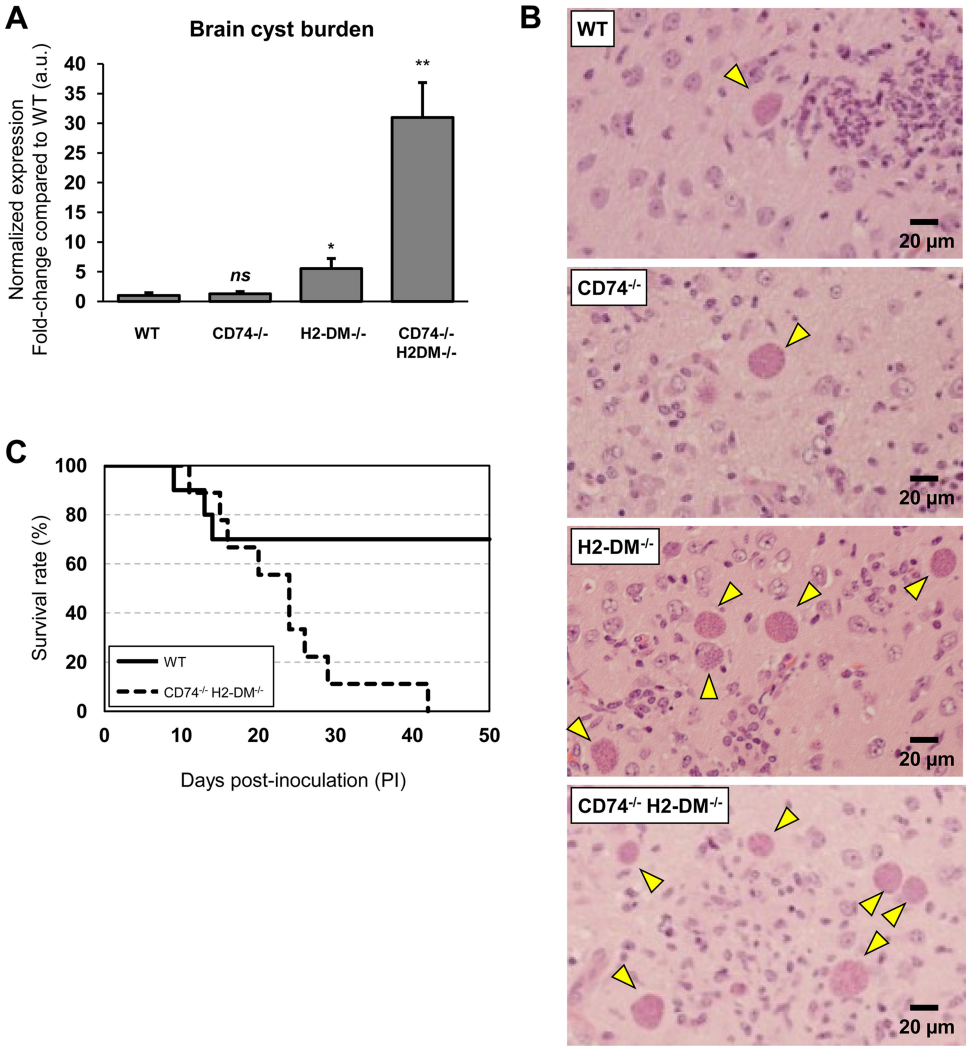

FIG 8 The absence of CD74 does not affect cyst numbers at the chronic stage of infection, while absence of H2-DM increases the burden and absence of both CD74 and H-2DM is fatal. (A) WT, CD74$^{-/-}$, H2-DM$^{-/-}$, and dKO (CD74$^{-/-}$ H2-DM$^{-/-}$) mice were infected i.p. with 10^3 PruΔ tachyzoites. Brains were collected 20 days p.i., and RT-PCR analysis using the *T. gondii* B1 gene was carried out to assess the relative cyst loads. The values shown were obtained from one representative infection trial out of three. The error bars indicate SD calculated from values obtained from three infected mice (for each strain). Significance was calculated using Student's *t* test (*ns*, not significant; *, $P < 0.05$; **, $P < 0.01$). Cyst counts at various time points yielded similar results. (B) Brains of infected animals were collected 10, 15, 20, and 25 days p.i.; prepared for histological sectioning; stained with hematoxylin and eosin; and observed by microscopy. Counting lesions was originally considered, given their higher recurrence in WT mice; however, the results were found to be variable. The arrowheads indicate cysts within brain tissue 25 days p.i. (C) WT and dKO mice were infected i.p. with 10^3 PruΔ tachyzoites, and the survival of the mice was monitored for 50 days. Infection trials included five mice per strain.

induction was not observed with phagocytosed dead parasites or parasite lysates, nor did it occur in uninfected bystander cells. These observations contrast with the mechanism of decreased MHC-II expression, since MHC-II is inhibited to a certain extent in uninfected bystander cells within infected cultures (14), and parasite lysates (33) and excreted-secreted antigens (66) directly display inhibitory activity.

There is significant evidence of differences in the modulation of the immune responses and signaling pathways by virulent type I and avirulent type II strains of *T. gondii*. Polymorphisms in secreted rhoptry and dense granule proteins, such as ROP16, ROP18, and GRA15, have been linked to differences in virulence and to differential modulation of immune-related functions (18, 63, 67). According to our results, both the type I and II strains tested elicited heightened CD74 expression during infection, which suggests that the molecules that upregulate CD74 do not display significant function-altering polymorphisms.

CD74 at the cell surface also acts as a receptor for MIF, and the binding of MIF initiates the MAPK signaling pathway (59). CD74 molecules accumulated intracellularly, but not at the surfaces of *T. gondii*-infected cells, making it unlikely that MIF signaling is enhanced. It was reported that MIF$^{-/-}$ mice are more susceptible to toxoplasmosis, suffer greater liver damage, harbor more brain cysts, and produce fewer proinflammatory cytokines (68). Surprisingly, CD74$^{-/-}$ mice were not more susceptible to toxoplasmosis; the potential benefits of lacking CD74 may have outweighed the detrimental effects of an impaired MIF-induced response.

Results obtained from the *in vitro* Eα antigen/YAe antibody system suggest that accumulation of CD74 in infected BMDCs coincides with the inhibition of endogenously acquired parasite-derived antigen presentation on MHC-II molecules. A direct effect of the accumulation of CD74 in infected cells would represent, to our knowledge, a novel mechanism of subversion of MHC-II antigen presentation by an intracellular protozoan. MHC-II-restricted antigen presentation of both exogenous and endogenous parasite-derived antigens was significantly impaired in the absence H2-DM. In light of these results, it appears that *T. gondii* induces two opposing patterns: CD74 overexpression and negative effects on parasite-derived peptide presentation within infected cells and generalized inhibition of MHC-II and H2-DM expression.

Although the precise mechanism by which CD74 blocks the presentation of endogenous parasite-derived antigens remains unknown, presentation of endogenous antigens from the cytosol or other compartments on MHC-II molecules has been demonstrated and involves autophagy or TAP-mediated mechanisms (69, 70). An accumulation of CD74 in infected cells could potentially affect the delivery to or loading of antigens onto MHC-II molecules. In the absence of CD74, the grooves of newly synthesized MHC-II molecules are left vacant and may bind to peptides derived from the ER that are not normally presented. Of note, *T. gondii* antigens can be detected in the ER of infected host cells (71). A study with CD74$^{-/-}$ mice showed that lack of CD74 facilitates the presentation of endogenously synthesized peptides by splenic pAPCs (72). Furthermore, mass spectrometry analyses of MHC-II-bound peptides from CD74-negative and CD74-expressing pAPCs revealed differences in the antigen repertoires (73). It is possible that the Eα-RFP fusion protein, either secreted (*ptub*P30-Eα-RFP) or released from the parasite's cytoplasm (*ptub*Eα-RFP) into the PV during replication, could have found its way into the host ER and could have been made available for loading onto MHC-II in the absence of CD74.

It has been proposed that the isoform composition of the CD74 trimers and the number of MHC-II αβ dimers that associate with the CD74 complexes determine the trafficking of MHC-II molecules (74). If fewer than three αβ dimers associate, the ER retention motif found in the cytoplasmic tail of CD74 prevents egress of MHC-II from the ER; CD74 overexpression could prevent trafficking of the small amount of MHC-II present in *T. gondii*-infected cells. Other studies have shown that endosomal trafficking is altered in cells expressing high levels of CD74 (75, 76), and perturbed trafficking may affect antigen delivery to late endocytic compartments and its processing and, consequently, antigen loading on MHC-II molecules.

We measured significantly higher parasite loads in the MLN of both CD74$^{-/-}$ and dKO mice than in WT or H2-DM$^{-/-}$ mice during the acute phase of infection. The increased parasite numbers did not seem to be important for enhanced parasite replication, since no differences were observed in the replication rates of tachyzoites *in vitro* in infected WT and CD74$^{-/-}$ BMMϕ (see Fig. S4 in the supplemental material). The total numbers of tachyzoites during the acute phase were possibly similar, but the dissemination pattern of *T. gondii*-infected cells toward lymphoid organs differed in animals lacking CD74. Faure-André and colleagues have demonstrated that CD74 interacts with the actin-based motor protein myosin II and affects cell motility in dendritic cells (77). WT DCs were found to alternate between high and low motility, while CD74$^{-/-}$ DCs moved in a faster and uniform fashion (77). Consequently, CD74 negatively regulates DC motility, perhaps, to allow more efficient sampling of antigens in the environment. Another study showed that IFN-α and IFN-γ synergistically act with Toll-like receptor (TLR) agonists to downregulate CD74 and thus confer high migratory capacity on mature DCs (78). In this regard, increased CD74 levels may delay trafficking of *T. gondii*-infected cells to lymphoid organs, where an adequate immune response can be mounted.

In the absence of CD74 and the peptide editor H2-DM, chronic infections with an avirulent *T. gondii* strain became invariably lethal, suggesting that CD74 and H2-DM may prevent a normal chronic infection from becoming lethal. Brain cyst numbers were similar in WT and CD74$^{-/-}$ mice at the chronic phase of infection, while cyst burdens increased ~6-fold in H2-DM$^{-/-}$ mice. Mortality rates were not increased, however, in H2-DM$^{-/-}$ mice. In contrast, brain cyst burdens in dKO mice were markedly elevated (~30-fold), and these mice exhibited neurological symptoms early during chronic infection and succumbed to lethal chronic infection. At this time, we cannot reject the possibility that tachyzoites that had not converted to bradyzoites were still circulating within these compromised dKO mice, contributing to the heightened mortality rate. Further experiments are required to examine this possibility. The precise mechanisms underlying the heightened mortality rates in double-KO mice remain elusive, but defective or perturbed CD4$^+$ T cell development, as shown by lower total CD3ε$^+$ CD4$^+$ T cell counts observed in the KO strains during acute infections (expansion) and as reported for CD74$^{-/-}$ (41), H2-DM$^{-/-}$ (42, 79), and CD74$^{-/-}$ H2-DM$^{-/-}$ (80) naive mice, would significantly change the outcome of toxoplasmosis (7–9). Thus, the differences in immune responses during acute infection and the higher number of cysts at the chronic phase in the mouse strains lacking H2-DM might be linked to a developmental CD4$^+$ T cell defect.

Collectively, our results show that *T. gondii* modulates MHC-II-restricted antigen presentation through multiple mechanisms, including transcriptional inhibition of IFN-γ-induced class II genes (MHC-II and H2-DM) and induction of CD74 expression within infected professional antigen-presenting cells. Overall, these immune subversion strategies would assist the parasite to establish a successful chronic infection.

ACKNOWLEDGMENTS

We thank Elizabeth Bikoff (University of Oxford) and Jörg Fritz (McGill University) for providing marrow from C57BL/6 CD74$^{-/-}$ and TNF-α$^{-/-}$ mice, respectively; Armando Jardim (Institute of Parasitology, McGill University) for *L. donovani* promastigotes; and Hervé Le Moual (McGill University) for *S. enterica* Typhimurium 14028 bacteria. Also, we acknowledge Ellen Robey (University of California, Berkley) for her support and helpful discussions over the years. Finally, we thank Tatiana Scorza (Université du Québec à Montréal) for her invaluable input on the manuscript.

The initial discovery of the CD74 phenotype is attributed to M.N. F.S.D., L.-P.L., and M.N. conceived and designed the experiments. L.-P.L., M.N., and S.E.-H. performed the experiments. F.S.D., L.-P.L., M.N., and S.E.-H. analyzed the data. D.J.B. and B.A.F. contributed reagents/material/analysis tools. L.-P.L. and F.S.D. wrote the paper.

This work was supported by a Natural Sciences and Engineering Research Council (NSERC) of Canada Discovery Grant (RGPIN 341433), a March of Dimes Grant (6-FY11-356), and the Canada Foundation for Innovation (203600). F.S.D. was supported by the Canada Research

Chairs, L.P.L. was a recipient of the Lynden Laird Lyster Memorial Fellowship in Parasitology and a Fonds de Recherche Nature et Technologies (FQRNT) B2 doctoral research scholarship (149810), and M.N. was supported by a FQRNT B3 postdoctoral fellowship (128468). The funders had no role in the study design, data collection and analysis, decision to publish, or preparation of the manuscript.

REFERENCES

1. **Frenkel JK, Dubey JP, Miller NL.** 1970. Toxoplasma gondii in cats: fecal stages identified as coccidian oocysts. Science **167:**893–896. http://dx.doi.org/10.1126/science.167.3919.893.
2. **Dubey JP, Miller NL, Frenkel JK.** 1970. The Toxoplasma gondii oocyst from cat feces. J Exp Med **132:**636–662. http://dx.doi.org/10.1084/jem.132.4.636.
3. **Dubey JP.** 2004. Toxoplasmosis—a waterborne zoonosis. Vet Parasitol **126:**57–72. http://dx.doi.org/10.1016/j.vetpar.2004.09.005.
4. **Dubey JP, Speer CA, Shen SK, Kwok OC, Blixt JA.** 1997. Oocyst-induced murine toxoplasmosis: life cycle, pathogenicity, and stage conversion in mice fed Toxoplasma gondii oocysts. J Parasitol **83:**870–882. http://dx.doi.org/10.2307/3284282.
5. **Montoya JG, Remington JS.** 2008. Management of Toxoplasma gondii infection during pregnancy. Clin Infect Dis **47:**554–566. http://dx.doi.org/10.1086/590149.
6. **Luft BJ, Remington JS.** 1992. Toxoplasmic encephalitis in AIDS. Clin Infect Dis **15:**211–222. http://dx.doi.org/10.1093/clinids/15.2.211.
7. **Gazzinelli RT, Hakim FT, Hieny S, Shearer GM, Sher A.** 1991. Synergistic role of CD4+ and CD8+ T lymphocytes in IFN-gamma production and protective immunity induced by an attenuated Toxoplasma gondii vaccine. J Immunol **146:**286–292.
8. **Suzuki Y, Orellana MA, Schreiber RD, Remington JS.** 1988. Interferon-gamma: the major mediator of resistance against Toxoplasma gondii. Science **240:**516–518. http://dx.doi.org/10.1126/science.3128869.
9. **Denkers EY, Gazzinelli RT.** 1998. Regulation and function of T-cell-mediated immunity during Toxoplasma gondii infection. Clin Microbiol Rev **11:**569–588.
10. **Shapira S, Harb OS, Margarit J, Matrajt M, Han J, Hoffmann A, Freedman B, May MJ, Roos DS, Hunter CA.** 2005. Initiation and termination of NF-kappaB signaling by the intracellular protozoan parasite Toxoplasma gondii. J Cell Sci **118:**3501–3508. http://dx.doi.org/10.1242/jcs.02428.
11. **Kim L, Butcher BA, Denkers EY.** 2004. Toxoplasma gondii interferes with lipopolysaccharide-induced mitogen-activated protein kinase activation by mechanisms distinct from endotoxin tolerance. J Immunol **172:**3003–3010. http://dx.doi.org/10.4049/jimmunol.172.5.3003.
12. **Zimmermann S, Murray PJ, Heeg K, Dalpke AH.** 2006. Induction of suppressor of cytokine signaling-1 by Toxoplasma gondii contributes to immune evasion in macrophages by blocking IFN-gamma signaling. J Immunol **176:**1840–1847. http://dx.doi.org/10.4049/jimmunol.176.3.1840.
13. **Lang C, Hildebrandt A, Brand F, Opitz L, Dihazi H, Luder CG.** 2012. Impaired chromatin remodelling at STAT1-regulated promoters leads to global unresponsiveness of Toxoplasma gondii-infected macrophages to IFN-gamma. PLoS Pathog **8:**e1002483. http://dx.doi.org/10.1371/journal.ppat.1002483.
14. **Stutz A, Kessler H, Kaschel ME, Meissner M, Dalpke AH.** 2012. Cell invasion and strain dependent induction of suppressor of cytokine signaling-1 by Toxoplasma gondii. Immunobiology **217:**28–36. http://dx.doi.org/10.1016/j.imbio.2011.08.008.
15. **Luder CG, Lang C, Giraldo-Velasquez M, Algner M, Gerdes J, Gross U.** 2003. Toxoplasma gondii inhibits MHC class II expression in neural antigen-presenting cells by down-regulating the class II transactivator CIITA. J Neuroimmunol **134:**12–24. http://dx.doi.org/10.1016/S0165-5728(02)00320-X.
16. **Butcher BA, Kim L, Panopoulos AD, Watowich SS, Murray PJ, Denkers EY.** 2005. IL-10-independent STAT3 activation by Toxoplasma gondii mediates suppression of IL-12 and TNF-alpha in host macrophages. J Immunol **174:**3148–3152. http://dx.doi.org/10.4049/jimmunol.174.6.3148.
17. **Ong YC, Reese ML, Boothroyd JC.** 2010. Toxoplasma rhoptry protein 16 (ROP16) subverts host function by direct tyrosine phosphorylation of STAT6. J Biol Chem **285:**28731–28740. http://dx.doi.org/10.1074/jbc.M110.112359.
18. **Jensen KD, Wang Y, Wojno ED, Shastri AJ, Hu K, Cornel L, Boedec E, Ong YC, Chien YH, Hunter CA, Boothroyd JC, Saeij JP.** 2011. Toxoplasma polymorphic effectors determine macrophage polarization and intestinal inflammation. Cell Host Microbe **9:**472–483. http://dx.doi.org/10.1016/j.chom.2011.04.015.
19. **Fentress SJ, Behnke MS, Dunay IR, Mashayekhi M, Rommereim LM, Fox BA, Bzik DJ, Taylor GA, Turk BE, Lichti CF, Townsend RR, Qiu W, Hui R, Beatty WL, Sibley LD.** 2010. Phosphorylation of immunity-related GTPases by a Toxoplasma gondii-secreted kinase promotes macrophage survival and virulence. Cell Host Microbe **8:**484–495. http://dx.doi.org/10.1016/j.chom.2010.11.005.
20. **Steinfeldt T, Konen-Waisman S, Tong L, Pawlowski N, Lamkemeyer T, Sibley LD, Hunn JP, Howard JC.** 2010. Phosphorylation of mouse immunity-related GTPase (IRG) resistance proteins is an evasion strategy for virulent Toxoplasma gondii. PLoS Biol **8:**e1000576. http://dx.doi.org/10.1371/journal.pbio.1000576.
21. **Niedelman W, Gold DA, Rosowski EE, Sprokholt JK, Lim D, Farid Arenas A, Melo MB, Spooner E, Yaffe MB, Saeij JP.** 2012. The rhoptry proteins ROP18 and ROP5 mediate Toxoplasma gondii evasion of the murine, but not the human, interferon-gamma response. PLoS Pathog **8:**e1002784. http://dx.doi.org/10.1371/journal.ppat.1002784.
22. **Luder CG, Lang T, Beuerle B, Gross U.** 1998. Down-regulation of MHC class II molecules and inability to up-regulate class I molecules in murine macrophages after infection with Toxoplasma gondii. Clin Exp Immunol **112:**308–316. http://dx.doi.org/10.1046/j.1365-2249.1998.00594.x.
23. **Luder CG, Walter W, Beuerle B, Maeurer MJ, Gross U.** 2001. Toxoplasma gondii down-regulates MHC class II gene expression and antigen presentation by murine macrophages via interference with nuclear translocation of STAT1alpha. Eur J Immunol **31:**1475–1484. http://dx.doi.org/10.1002/1521-4141(200105)31:5<1475::AID-IMMU1475>3.0.CO;2-C.
24. **McKee AS, Dzierszinski F, Boes M, Roos DS, Pearce EJ.** 2004. Functional inactivation of immature dendritic cells by the intracellular parasite Toxoplasma gondii. J Immunol **173:**2632–2640. http://dx.doi.org/10.4049/jimmunol.173.4.2632.
25. **Hudson AW, Ploegh HL.** 2002. The cell biology of antigen presentation. Exp Cell Res **272:**1–7. http://dx.doi.org/10.1006/excr.2001.5402.
26. **Roche PA, Marks MS, Cresswell P.** 1991. Formation of a nine-subunit complex by HLA class II glycoproteins and the invariant chain. Nature **354:**392–394. http://dx.doi.org/10.1038/354392a0.
27. **Lamb CA, Cresswell P.** 1992. Assembly and transport properties of invariant chain trimers and HLA-DR-invariant chain complexes. J Immunol **148:**3478–3482.
28. **Pieters J, Bakke O, Dobberstein B.** 1993. The MHC class II-associated invariant chain contains two endosomal targeting signals within its cytoplasmic tail. J Cell Sci **106:**831–846.
29. **Odorizzi CG, Trowbridge IS, Xue L, Hopkins CR, Davis CD, Collawn JF.** 1994. Sorting signals in the MHC class II invariant chain cytoplasmic tail and transmembrane region determine trafficking to an endocytic processing compartment. J Cell Biol **126:**317–330. http://dx.doi.org/10.1083/jcb.126.2.317.
30. **Kongsvik TL, Honing S, Bakke O, Rodionov DG.** 2002. Mechanism of interaction between leucine-based sorting signals from the invariant chain and clathrin-associated adaptor protein complexes AP1 and AP2. J Biol Chem **277:**16484–16488. http://dx.doi.org/10.1074/jbc.M201583200.
31. **Bonifacino JS, Traub LM.** 2003. Signals for sorting of transmembrane proteins to endosomes and lysosomes. Annu Rev Biochem **72:**395–447. http://dx.doi.org/10.1146/annurev.biochem.72.121801.161800.
32. **Hsing LC, Rudensky AY.** 2005. The lysosomal cysteine proteases in MHC class II antigen presentation. Immunol Rev **207:**229–241. http://dx.doi.org/10.1111/j.0105-2896.2005.00310.x.
33. **Lang C, Algner M, Beinert N, Gross U, Luder CG.** 2006. Diverse mechanisms employed by Toxoplasma gondii to inhibit IFN-gamma-induced major histocompatibility complex class II gene expression. Microbes Infect **8:**1994–2005. http://dx.doi.org/10.1016/j.micinf.2006.02.031.
34. **Kim SK, Fouts AE, Boothroyd JC.** 2007. Toxoplasma gondii dysregulates IFN-gamma-inducible gene expression in human fibroblasts: insights from a genome-wide transcriptional profiling. J Immunol **178:**5154–5165. http://dx.doi.org/10.4049/jimmunol.178.8.5154.
35. **Wei S, Marches F, Borvak J, Zou W, Channon J, White M, Radke J, Cesbron-Delauw MF, Curiel TJ.** 2002. Toxoplasma gondii-infected human myeloid dendritic cells induce T-lymphocyte dysfunction and con-

tact-dependent apoptosis. Infect Immun **70:**1750–1760. http://dx.doi.org/10.1128/IAI.70.4.1750-1760.2002.
36. **Subauste CS, Wessendarp M.** 2000. Human dendritic cells discriminate between viable and killed Toxoplasma gondii tachyzoites: dendritic cell activation after infection with viable parasites results in CD28 and CD40 ligand signaling that controls IL-12-dependent and -independent T cell production of IFN-gamma. J Immunol **165:**1498–1505. http://dx.doi.org/10.4049/jimmunol.165.3.1498.
37. **Reis e Sousa C, Hieny S, Scharton-Kersten T, Jankovic D, Charest H, Germain RN, Sher A.** 1997. In vivo microbial stimulation induces rapid CD40 ligand-independent production of interleukin 12 by dendritic cells and their redistribution to T cell areas. J Exp Med **186:**1819–1829. http://dx.doi.org/10.1084/jem.186.11.1819.
38. **Aliberti J, Reis e Sousa C, Schito M, Hieny S, Wells T, Huffnagle GB, Sher A.** 2000. CCR5 provides a signal for microbial induced production of IL-12 by CD8 alpha+ dendritic cells. Nat Immunol **1:**83–87. http://dx.doi.org/10.1038/76957.
39. **Scanga CA, Aliberti J, Jankovic D, Tilloy F, Bennouna S, Denkers EY, Medzhitov R, Sher A.** 2002. Cutting edge: MyD88 is required for resistance to Toxoplasma gondii infection and regulates parasite-induced IL-12 production by dendritic cells. J Immunol **168:**5997–6001. http://dx.doi.org/10.4049/jimmunol.168.12.5997.
40. **Aliberti J, Valenzuela JG, Carruthers VB, Hieny S, Andersen J, Charest H, Reis e Sousa C, Fairlamb A, Ribeiro JM, Sher A.** 2003. Molecular mimicry of a CCR5 binding-domain in the microbial activation of dendritic cells. Nat Immunol **4:**485–490. http://dx.doi.org/10.1038/ni915.
41. **Bikoff EK, Huang LY, Episkopou V, van Meerwijk J, Germain RN, Robertson EJ.** 1993. Defective major histocompatibility complex class II assembly, transport, peptide acquisition, and CD4+ T cell selection in mice lacking invariant chain expression. J Exp Med **177:**1699–1712. http://dx.doi.org/10.1084/jem.177.6.1699.
42. **Miyazaki T, Wolf P, Tourne S, Waltzinger C, Dierich A, Barois N, Ploegh H, Benoist C, Mathis D.** 1996. Mice lacking H2-M complexes, enigmatic elements of the MHC class II peptide-loading pathway. Cell **84:**531–541. http://dx.doi.org/10.1016/S0092-8674(00)81029-6.
43. **Roos DS, Donald RG, Morrissette NS, Moulton AL.** 1994. Molecular tools for genetic dissection of the protozoan parasite Toxoplasma gondii. Methods Cell Biol **45:**27–63.
44. **Fox BA, Bzik DJ.** 2002. De novo pyrimidine biosynthesis is required for virulence of Toxoplasma gondii. Nature **415:**926–929. http://dx.doi.org/10.1038/415926a.
45. **Itano AA, McSorley SJ, Reinhardt RL, Ehst BD, Ingulli E, Rudensky AY, Jenkins MK.** 2003. Distinct dendritic cell populations sequentially present antigen to CD4 T cells and stimulate different aspects of cell-mediated immunity. Immunity **19:**47–57. http://dx.doi.org/10.1016/S1074-7613(03)00175-4.
46. **Dzierszinski FS, Hunter CA.** 2008. Advances in the use of genetically engineered parasites to study immunity to Toxoplasma gondii. Parasite Immunol **30:**235–244. http://dx.doi.org/10.1111/j.1365-3024.2007.01016.x.
47. **Pepper M, Dzierszinski F, Wilson E, Tait E, Fang Q, Yarovinsky F, Laufer TM, Roos D, Hunter CA.** 2008. Plasmacytoid dendritic cells are activated by Toxoplasma gondii to present antigen and produce cytokines. J Immunol **180:**6229–6236. http://dx.doi.org/10.4049/jimmunol.180.9.6229.
48. **Weischenfeldt J, Porse B.** 2008. Bone marrow-derived macrophages (BMM): isolation and applications. CSH Protoc **2008:**pdb.prot5080. http://dx.doi.org/10.1101/pdb.prot5080.
49. **Lutz MB, Suri RM, Niimi M, Ogilvie AL, Kukutsch NA, Rossner S, Schuler G, Austyn JM.** 2000. Immature dendritic cells generated with low doses of GM-CSF in the absence of IL-4 are maturation resistant and prolong allograft survival in vivo. Eur J Immunol **30:**1813–1822. http://dx.doi.org/10.1002/1521-4141(200007)30:7<1813::AID-IMMU1813>3.0.CO;2-8.
50. **Murphy DB, Lo D, Rath S, Brinster RL, Flavell RA, Slanetz A, Janeway CA, Jr.** 1989. A novel MHC class II epitope expressed in thymic medulla but not cortex. Nature **338:**765–768. http://dx.doi.org/10.1038/338765a0.
51. **Schindelin J, Arganda-Carreras I, Frise E, Kaynig V, Longair M, Pietzsch T, Preibisch S, Rueden C, Saalfeld S, Schmid B, Tinevez JY, White DJ, Hartenstein V, Eliceiri K, Tomancak P, Cardona A.** 2012. Fiji: an open-source platform for biological-image analysis. Nat Methods **9:**676–682. http://dx.doi.org/10.1038/nmeth.2019.
52. **Livak KJ, Schmittgen TD.** 2001. Analysis of relative gene expression data using real-time quantitative PCR and the 2(-Delta Delta C(T)) method. Methods **25:**402–408. http://dx.doi.org/10.1006/meth.2001.1262.
53. **Burg JL, Grover CM, Pouletty P, Boothroyd JC.** 1989. Direct and sensitive detection of a pathogenic protozoan, Toxoplasma gondii, by polymerase chain reaction. J Clin Microbiol **27:**1787–1792.
54. **Lin MH, Chen TC, Kuo TT, Tseng CC, Tseng CP.** 2000. Real-time PCR for quantitative detection of Toxoplasma gondii. J Clin Microbiol **38:**4121–4125.
55. **Jauregui LH, Higgins J, Zarlenga D, Dubey JP, Lunney JK.** 2001. Development of a real-time PCR assay for detection of Toxoplasma gondii in pig and mouse tissues. J Clin Microbiol **39:**2065–2071. http://dx.doi.org/10.1128/JCM.39.6.2065-2071.2001.
56. **Reiner NE, Ng W, McMaster WR.** 1987. Parasite-accessory cell interactions in murine leishmaniasis. II. Leishmania donovani suppresses macrophage expression of class I and class II major histocompatibility complex gene products. J Immunol **138:**1926–1932.
57. **Kwan WC, McMaster WR, Wong N, Reiner NE.** 1992. Inhibition of expression of major histocompatibility complex class II molecules in macrophages infected with Leishmania donovani occurs at the level of gene transcription via a cyclic AMP-independent mechanism. Infect Immun **60:**2115–2120.
58. **Mitchell EK, Mastroeni P, Kelly AP, Trowsdale J.** 2004. Inhibition of cell surface MHC class II expression by Salmonella. Eur J Immunol **34:**2559–2567. http://dx.doi.org/10.1002/eji.200425314.
59. **Leng L, Metz CN, Fang Y, Xu J, Donnelly S, Baugh J, Delohery T, Chen Y, Mitchell RA, Bucala R.** 2003. MIF signal transduction initiated by binding to CD74. J Exp Med **197:**1467–1476. http://dx.doi.org/10.1084/jem.20030286.
60. **Pessara U, Koch N.** 1990. Tumor necrosis factor alpha regulates expression of the major histocompatibility complex class II-associated invariant chain by binding of an NF-kappa B-like factor to a promoter element. Mol Cell Biol **10:**4146–4154.
61. **Kolk DP, Floyd-Smith G.** 1993. Induction of the murine class-II antigen-associated invariant chain by TNF-alpha is controlled by an NF-kappa B-like element. Gene **126:**179–185. http://dx.doi.org/10.1016/0378-1119(93)90365-A.
62. **Nistico P, Tecce R, Giacomini P, Cavallari A, D'Agnano I, Fisher PB, Natali PG.** 1990. Effect of recombinant human leukocyte, fibroblast, and immune interferons on expression of class I and II major histocompatibility complex and invariant chain in early passage human melanoma cells. Cancer Res **50:**7422–7429.
63. **Saeij JP, Boyle JP, Coller S, Taylor S, Sibley LD, Brooke-Powell ET, Ajioka JW, Boothroyd JC.** 2006. Polymorphic secreted kinases are key virulence factors in toxoplasmosis. Science **314:**1780–1783. http://dx.doi.org/10.1126/science.1133690.
64. **Glimcher LH, Kara CJ.** 1992. Sequences and factors: a guide to MHC class-II transcription. Annu Rev Immunol **10:**13–49. http://dx.doi.org/10.1146/annurev.iy.10.040192.000305.
65. **Zhu L, Jones PP.** 1990. Transcriptional control of the invariant chain gene involves promoter and enhancer elements common to and distinct from major histocompatibility complex class II genes. Mol Cell Biol **10:**3906–3916.
66. **Leroux LP, Dasanayake D, Rommereim LM, Fox BA, Bzik DJ, Jardim A, Dzierszinski FS.** 2015. Secreted Toxoplasma gondii molecules interfere with expression of MHC-II in interferon gamma-activated macrophages. Int J Parasitol **45:**319–332. http://dx.doi.org/10.1016/j.ijpara.2015.01.003.
67. **Butcher BA, Fox BA, Rommereim LM, Kim SG, Maurer KJ, Yarovinsky F, Herbert DR, Bzik DJ, Denkers EY.** 2011. Toxoplasma gondii rhoptry kinase ROP16 activates STAT3 and STAT6 resulting in cytokine inhibition and arginase-1-dependent growth control. PLoS Pathog **7:**e1002236. http://dx.doi.org/10.1371/journal.ppat.1002236.
68. **Flores M, Saavedra R, Bautista R, Viedma R, Tenorio EP, Leng L, Sanchez Y, Juarez I, Satoskar AA, Shenoy AS, Terrazas LI, Bucala R, Barbi J, Satoskar AR, Rodriguez-Sosa M.** 2008. Macrophage migration inhibitory factor (MIF) is critical for the host resistance against Toxoplasma gondii. FASEB J **22:**3661–3671. http://dx.doi.org/10.1096/fj.08-111666.
69. **Trombetta ES, Mellman I.** 2005. Cell biology of antigen processing in vitro and in vivo. Annu Rev Immunol **23:**975–1028. http://dx.doi.org/10.1146/annurev.immunol.22.012703.104538.
70. **Munz C.** 2004. Epstein-Barr virus nuclear antigen 1: from immunologically invisible to a promising T cell target. J Exp Med **199:**1301–1304. http://dx.doi.org/10.1084/jem.20040730.

71. **Goldszmid RS, Coppens I, Lev A, Caspar P, Mellman I, Sher A.** 2009. Host ER-parasitophorous vacuole interaction provides a route of entry for antigen cross-presentation in Toxoplasma gondii-infected dendritic cells. J Exp Med **206:**399–410. http://dx.doi.org/10.1084/jem.20082108.
72. **Bodmer H, Viville S, Benoist C, Mathis D.** 1994. Diversity of endogenous epitopes bound to MHC class II molecules limited by invariant chain. Science **263:**1284–1286. http://dx.doi.org/10.1126/science.7510069.
73. **Muntasell A, Carrascal M, Alvarez I, Serradell L, van Veelen P, Verreck FA, Koning F, Abian J, Jaraquemada D.** 2004. Dissection of the HLA-DR4 peptide repertoire in endocrine epithelial cells: strong influence of invariant chain and HLA-DM expression on the nature of ligands. J Immunol **173:**1085–1093. http://dx.doi.org/10.4049/jimmunol.173.2.1085.
74. **Cresswell P, Roche PA.** 2014. Invariant chain-MHC class II complexes: always odd and never invariant. Immunol Cell Biol **92:**471–472. http://dx.doi.org/10.1038/icb.2014.36.
75. **Romagnoli P, Layet C, Yewdell J, Bakke O, Germain RN.** 1993. Relationship between invariant chain expression and major histocompatibility complex class II transport into early and late endocytic compartments. J Exp Med **177:**583–596. http://dx.doi.org/10.1084/jem.177.3.583.
76. **Gregers TF, Nordeng TW, Birkeland HC, Sandlie I, Bakke O.** 2003. The cytoplasmic tail of invariant chain modulates antigen processing and presentation. Eur J Immunol **33:**277–286. http://dx.doi.org/10.1002/immu.200310001.
77. **Faure-André G, Vargas P, Yuseff MI, Heuze M, Diaz J, Lankar D, Steri V, Manry J, Hugues S, Vascotto F, Boulanger J, Raposo G, Bono MR, Rosemblatt M, Piel M, Lennon-Dumenil AM.** 2008. Regulation of dendritic cell migration by CD74, the MHC class II-associated invariant chain. Science **322:**1705–1710. http://dx.doi.org/10.1126/science.1159894.
78. **Nguyen-Pham TN, Lim MS, Nguyen TA, Lee YK, Jin CJ, Lee HJ, Hong CY, Ahn JS, Yang DH, Kim YK, Chung IJ, Park BC, Kim HJ, Lee JJ.** 2011. Type I and II interferons enhance dendritic cell maturation and migration capacity by regulating CD38 and CD74 that have synergistic effects with TLR agonists. Cell Mol Immunol **8:**341–347. http://dx.doi.org/10.1038/cmi.2011.7.
79. **Bikoff EK, Kenty G, Van Kaer L.** 1998. Distinct peptide loading pathways for MHC class II molecules associated with alternative Ii chain isoforms. J Immunol **160:**3101–3110.
80. **Kovats S, Grubin CE, Eastman S, deRoos P, Dongre A, Van Kaer L, Rudensky AY.** 1998. Invariant chain-independent function of H-2M in the formation of endogenous peptide-major histocompatibility complex class II complexes in vivo. J Exp Med **187:**245–251. http://dx.doi.org/10.1084/jem.187.2.245.